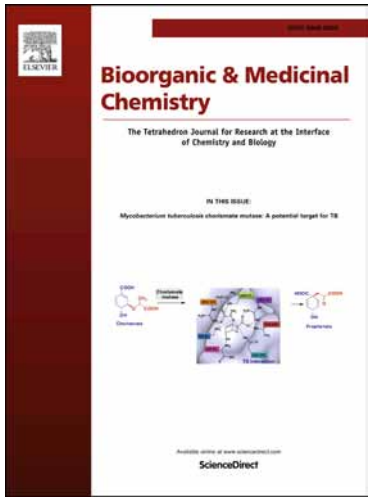

Design and Synthesis of Quinazolinones as EGFR inhibitors to Overcome EGFR Resistance Obstacle

Harun M. Patel, Rahul Pawara, Azim Ansari, Malleshappa Noolvi, Sanjay Surana

PII: S0968-0896(17)30036-6
DOI: http://dx.doi.org/10.1016/j.bmc.2017.03.039
Reference: BMC 13637

To appear in: *Bioorganic & Medicinal Chemistry*

Received Date: 9 January 2017
Revised Date: 14 March 2017
Accepted Date: 16 March 2017

Please cite this article as: Patel, H.M., Pawara, R., Ansari, A., Noolvi, M., Surana, S., Design and Synthesis of Quinazolinones as EGFR inhibitors to Overcome EGFR Resistance Obstacle, *Bioorganic & Medicinal Chemistry* (2017), doi: http://dx.doi.org/10.1016/j.bmc.2017.03.039

Design and Synthesis of Quinazolinones as EGFR inhibitors to Overcome EGFR Resistance Obstacle

Harun M. Patel [a] *, Rahul Pawara [a], Azim Ansari [a], Malleshappa Noolvi [b], Sanjay Surana [a]

[a] Department of Pharmaceutical Chemistry, R. C. Patel Institute of Pharmaceutical Education and Research, Shirpur, District Dhule-425 405, Maharashtra, India

[b] Department of Pharmaceutical Chemistry, Shree Dhanvantary Pharmacy College, Kim (Surat)-3941110, Gujrat, India

Corresponding Author*

Tel: +91-8806621544; Email:hpatel_38@yahoo.com

Abstract

The epidermal growth factor receptor (EGFR) T790M mutant is found in about 50% of clinically acquired resistance to gefitinib among patients with non-small cell lung cancer (NSCLC). New derivatives of 4(3*H*)-quinazolinones were synthesized and evaluated for their inhibitory activity against NSCLC. The results of the study demonstrated that compound **79**, 7-chloro-3-(5-(4-methoxyphenyl)-1,3,4-thiadiazol-2-yl)-2-phenylquinazolin-4(3*H*)-one was found to be the most potent compounds of the series with IC_{50} value of 0.031 μM against mutant T790M/L858R EGFR. Compounds **15**, **51**, **73**, **75**, **78**, **79** and **96** were less potent against A549 (WT EGFR and k-Ras mutation) and HT-29 (non-special gene type) cells, showing a high safety index. The obtained results showed that compounds **15**, **51**, **73**, **75**, **78**, **79** and **96** could be the promising template to overcome drug resistance mediated by the EGFR T790 Mutant.

Keywords: Quinazoline; Non Small Cell Lung Cancer, T790M EGFR

1. Introduction

The role of the epidermal growth factor receptor (EGFR) in non small-cell lung cancer (NSCLC) is well-known, and considerable therapeutic progress in the treatment of this disease has made over thepast 10 years through the exploitation of this insight.[1,2] The epidermal growth factor receptor (EGFR) has been established as one of the most important therapeutic targets for NSCLC. [3,4] Two small-molecule inhibitors of EGFR, gefitinib and erlotinib, have been approved by the U.S. Food and Drug Administration (FDA) for the treatment of NSCLC. [5-8] Gefitinib and erlotinib (**Fig. 1**), as the first generation ATP-competitive and reversible EGFR inhibitors, were effective for NSCLC patients harbouring somatic EGFR mutations L858R and delE746_A750 which account for 90% of all EGFR mutations in NSCLC. [9] Unfortunately, due to acquired secondary mutations such as T790M missense in EGFR leading to drug resistance in roughly 50% NSCLC patients, the ability of these EGFR inhibitors to effectively treat NSCLC patients is short-lived to later treatments. [10,11] EGFR T790M mutation restores the affinity for ATP similar to that of wild type (WT) EGFR, and prevents the reversible inhibitors from binding at higher ATP concentrations. [12]

Second generation EGFR inhibitors such as canertinib [13], afatinib [14], neratinib [15], and dacomitinib [16] (**Fig. 1**) have been developed with intent to overcome the T790M mutation related resistance.[17] The molecules of these inhibitors are built based on a quinazoline or quinoline core scaffold like gefitinib and erlotinib, but contain an electrophilic functionality that can undergoes a Micheal addition reaction with a conserved cysteine residue present in EGFR (Cys797) to get occupancy greater than that of the reversible inhibitors. [17] However, since the ATP affinity of EGFR T790M is similar to that of WT EGFR, these EGFR inhibitors at the concentrations required to inhibit EGFR T790M will also effectively inhibit WT EGFR, leading to the dose-limiting toxicity such as diarrhoea and skin rash.

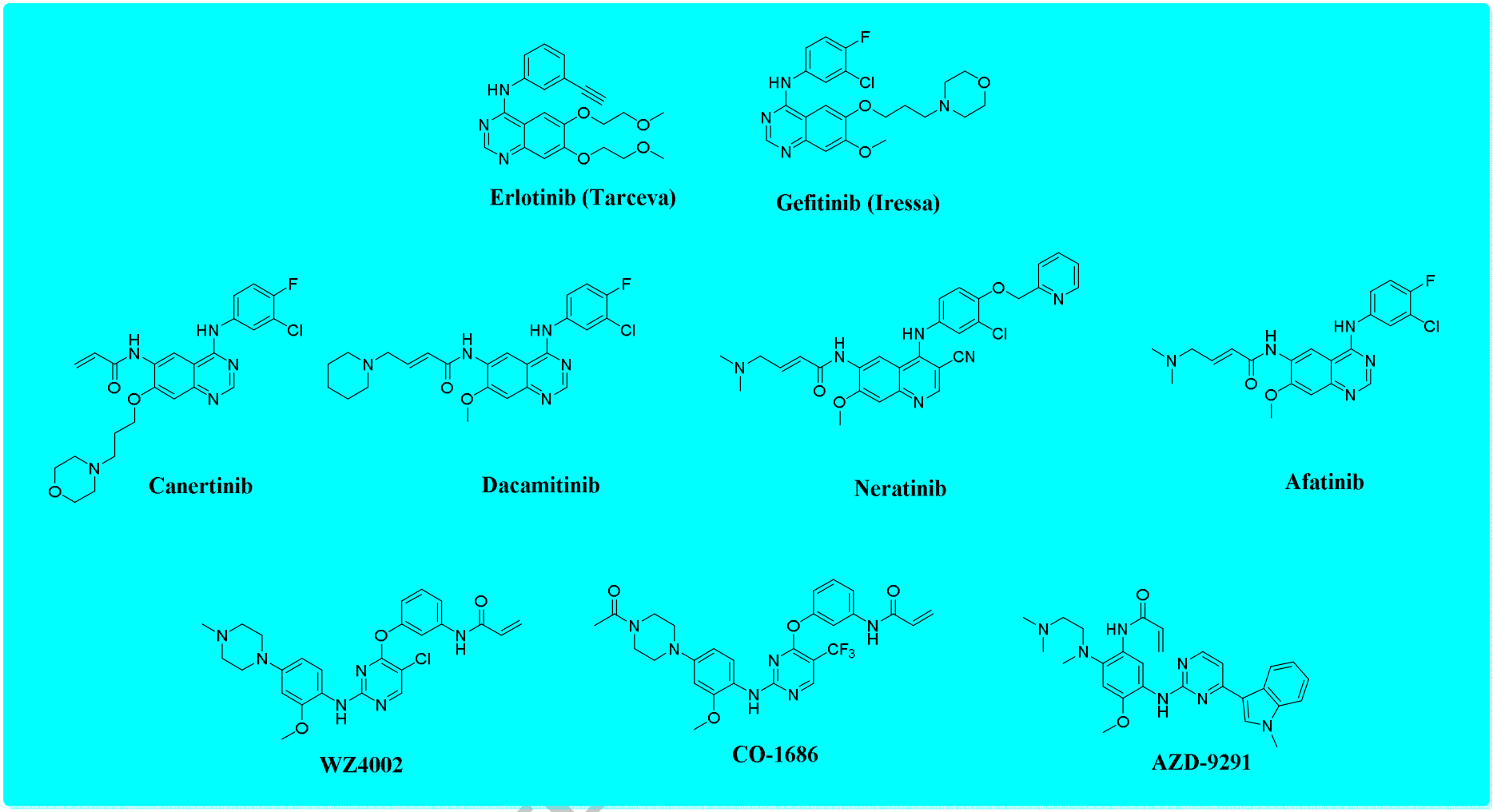

Fig. 1. First, second and third generation EGFR inhibitors.

Therefore, the clinical application of these inhibitors has been limited, especially in patients with gefitinib or erlotinib-resistant NSCLC. Hence the EGFR NSCLC inhibitors developed with less efficacy against WT EGFR has become a significant unmet need for the treatments of NSCLC patients.

2. Rationale

Third generation irreversible EGFR inhibitors containing a Michael acceptor functional group have been developed to overcome the problem of second generation irreversible inhibitors with minimal WT EGFR activity and enhanced ATP binding by irreversibly alkylating a cysteine residue (C797) in the ATP binding site of the EGFR.[18-26] However, except for a few examples, such as PF00299804,[27] and WZ-4002,[28] these irreversible inhibitors have thus far shown limited clinical efficacy. Inherent weaknesses, including relatively high toxicity and a decreased binding rate to the mutant kinase, may be responsible for the lack of clinical efficacy.[29-31] There has been a recent report of C797S mutation or loss of the T790M mutation in cell-free plasma DNA samples from patients who have developed resistance, [32] and a second separate report of C797S mutation in biopsy samples from a single patient .[33] Additionally, studies with third-generation resistant cell lines have shown that the allelic context of the activating gatekeeper and C797S mutations affects the sensitivity to the three generations of inhibitors with no EGFR TKIs alone or in combination able to suppress activity when the mutations are in cis.[34] These data suggest that there is a need for drugs which do not rely on covalent reaction with Cys797 for potency or selectivity.

In view of this justification and in continuation of an ongoing program aiming at finding new structure leads with potential chemotherapeutic activities [35-38], in the present study new series of quinazolinones have been synthesized, which comprises the 2,3-disubstituted quinazoline pharmacophore (**Fig. 2**).

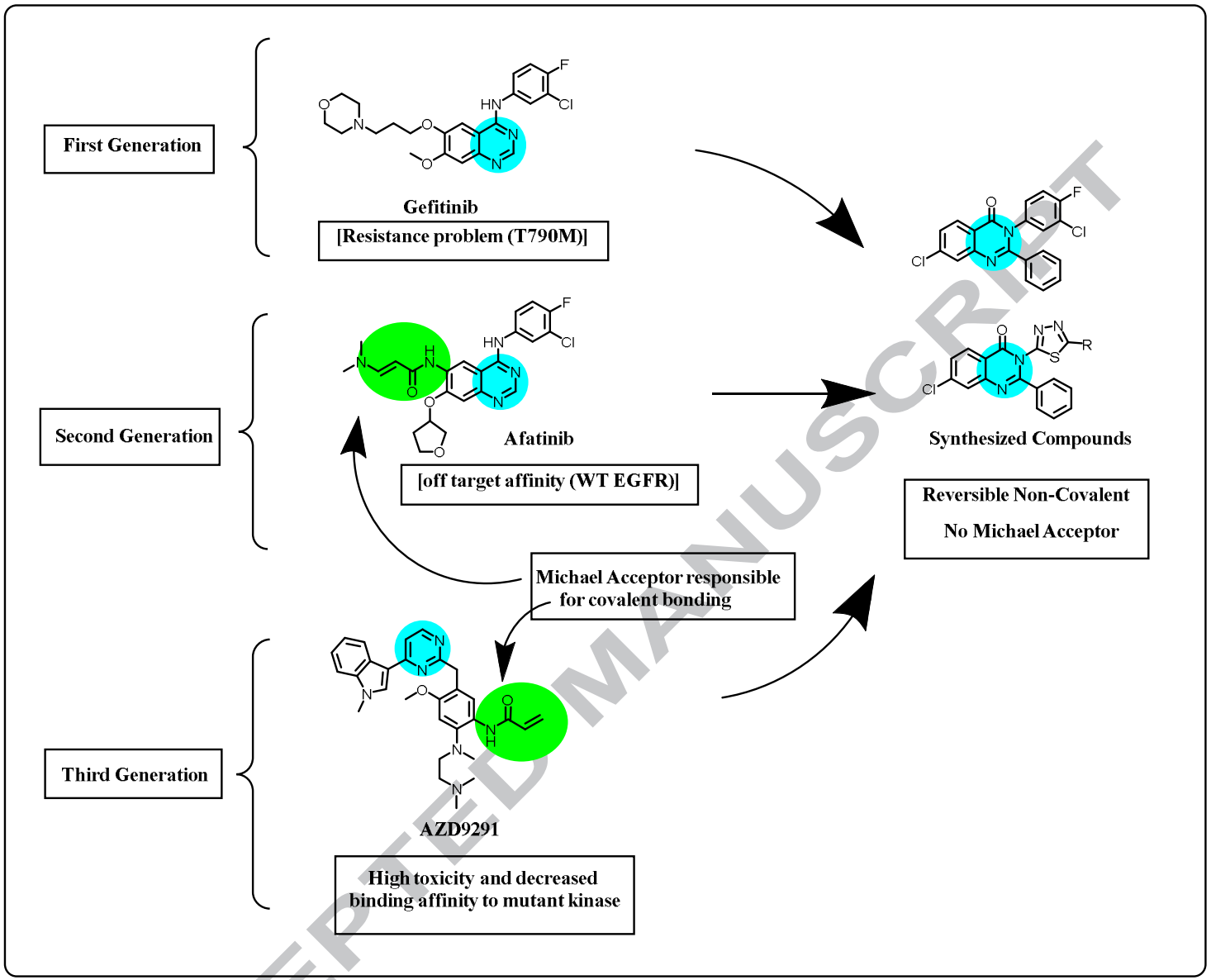

Fig. 2. Rationale for the designing of new scaffold.

Our strategy directs toward designing a variety of ligands with diverse chemical properties hypothesizing that the potency of these molecules might be enhanced by adding alternative binding group such as phenyl ring at place C-2, aniline with electron withdrawing groups, 2-amino thiadiazoles and different primary amine containing motifs at position 3-of the quinazoline ring. We intensely didn't introduce Michel acceptor to avoid the covalent binding. In this way, such substitution pattern could target different regions of the ATP-binding site of the T790M EGFR protein kinase domain as compare to the existing first, second and third generation agent to create differentially selective molecules.

3. Chemistry

Anthranilic acid **1a, 1b** reaction with benzoyl chloride **2**, yielded 2-phenyl-4*H*-3,1-benzoxazin-4 one **3a** and 7-chloro 2-phenyl-4*H*-3,1-benzoxazin-4 one **3b** by *N*-acylation *via* dehydrative cyclization mechanism as reported in our previous paper.[39] The reaction of different primary amines containing anilines, sulphonamides, thiadiazoles and hydrazides with 2-phenyl-4*H*-3,1-benzoxazin-4 one **3a** and 7-chloro 2-phenyl-4*H*-3,1-benzoxazin-4 one **3b** in dry pyridine yielded the corresponding quinazoline-4-one derivatives as shown in **Scheme 1.** It observed that while synthesizing the compounds **16, 19, 20, 63-66, 70, 71, 74, 86, 92, 93, 95, 97-103** by fusion reaction in an attempt to obtain 3-substituted-quinazolin-4-ones in different reaction conditions; the reaction afforded the (ring open quinazolines) diamides **(Scheme 1**). It could have happend because of ring opening tendancy of benzoxazinones with different nucleophiles, allowing incorporation of substitution at the 3-position.[39]

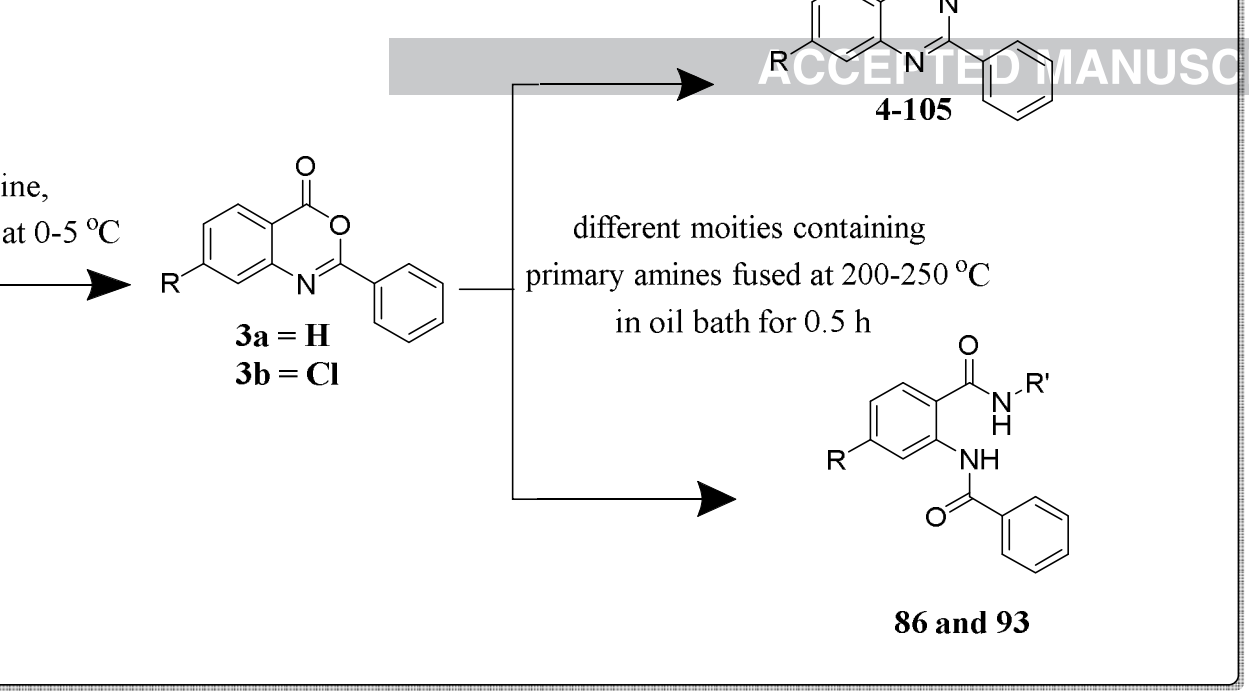

R	Compound Code	R'	R	Compound Code	R'	R
Cl	**73**	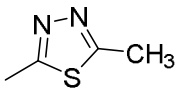	Cl	**86**	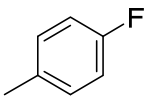	Cl
Cl	**75**	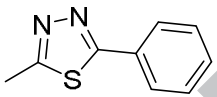	Cl	**93**	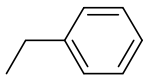	Cl
Cl	**78**	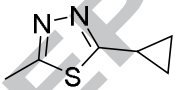	Cl	**94**	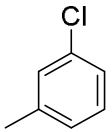	Cl
Cl	**79**	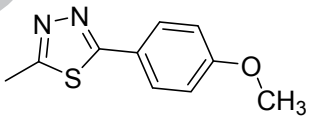	Cl	**96**	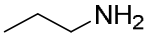	Cl

4. Pharmacology

4.1 In vitro cancer screen

The screening is a two-stage process, beginning with the evaluation of all compounds against the 60 cell lines at a single dose of 10^{-5}M.

The output from the single dose screen is reported as a mean graph and is available for analysis by the COMPARE program. Compounds which exhibit significant growth inhibition are evaluated against the 60 cell panel at five concentration levels. The human tumor cell lines of the cancer screening panel are grown in RPMI 1640 medium containing 5% fetal bovine serum and 2 mM L-glutamine. For a typical screening experiment, cells are inoculated into 96 well microtiter plates in 100 µL at plating densities ranging from 5,000 to 40,000 cells/well depending on the doubling time of individual cell lines. After cell inoculation, the microtiter plates are incubated at 37°C, 5 % CO_2, 95 % air and 100 % relative humidity for 24 h prior to addition of experimental drugs. After 24 h, two plates of each cell line are fixed *in situ* with TCA, to represent a measurement of the cell population for each cell line at the time of drug addition (Tz). Experimental drugs are solubilized in dimethyl sulfoxide at 400-fold the desired final maximum test concentration and stored frozen prior to use. At the time of drug addition, an aliquot of frozen concentrate is thawed and diluted to twice the desired final maximum test concentration with complete medium containing 50 µg/ml gentamicin. Additional four, 10-fold or ½ log serial dilutions are made to provide a total of five drug concentrations plus control. Aliquots of 100 µl of these different drug dilutions are added to the appropriate microtiter wells already containing 100 µl of medium, resulting in the required final drug concentrations.

Following drug addition, the plates are incubated for an additional 48 h at 37°C, 5 % CO_2, 95 % air, and 100 % relative humidity. For adherent cells, the assay is terminated by the addition of

cold TCA. Cells are fixed *in situ* by the gentle addition of 50 µl of cold 50 % (w/v) TCA (final concentration, 10 % TCA) and incubated for 60 minutes at 4°C. The supernatant is discarded, and the plates are washed five times with tap water and air dried. Sulforhodamine B (SRB) solution (100 µl) at 0.4 % (w/v) in 1 % acetic acid is added to each well, and plates are incubated for 10 minutes at room temperature. After staining, unbound dye is removed by washing five times with 1 % acetic acid and the plates are air dried. Bound stain is subsequently solubilized with 10 mM trizma base, and the absorbance is read on an automated plate reader at a wavelength of 515 nm. For suspension cells, the methodology is the same except that the assay is terminated by fixing settled cells at the bottom of the wells by gently adding 50 µl of 80 % TCA (final concentration, 16 % TCA). Using the seven absorbance measurements [time zero, (Tz), control growth, (C), and test growth in the presence of drug at the five concentration levels (Ti)], the percentage growth is calculated at each of the drug concentrations levels. Percentage growth inhibition is calculated as:

$$[(Ti-Tz)/(C-Tz)] \times 100 \text{ for concentrations for which } Ti \geq Tz$$

$$[(Ti-Tz)/Tz] \times 100 \text{ for concentrations for which } Ti < Tz.$$

Three dose response parameters are calculated for each experimental agent. Growth inhibition of 50 % (GI50) is calculated from $[(Ti-Tz)/(C-Tz)] \times 100 = 50$, which is the drug concentration resulting in a 50 % reduction in the net protein increase (as measured by SRB staining) in control cells during the drug incubation. The drug concentration resulting in total growth inhibition (TGI) is calculated from Ti = Tz. The LC_{50} (concentration of drug resulting in a 50 % reduction in the measured protein at the end of the drug treatment as compared to that at the beginning) indicating a net loss of cells following treatment is calculated from $[(Ti-Tz)/Tz] \times 100 = -50$. Values are calculated for each of these three parameters if the level of activity is reached; however, if the

effect is not reached or is exceeded, the value for that parameter is expressed as greater or less than the maximum or minimum concentration tested. [40-43]

4.1.2 Primary single high dose (10^{-5}M) full NCI 60 cell panel in vitro assay

All the selected compounds submitted to National Cancer Institute (NCI) for *in vitro* anticancer assay were evaluated for their anticancer activity. Primary *in vitro* one dose anticancer assay was performed in full NCI 60 cell panel representing leukemia, melanoma and cancers of lung, colon brain breast, ovary, kidney and prostate in accordance with the protocol of the NCI, USA. The compounds were added at a single concentration (10^{-5}M) and the culture was incubated for 48 h. End point determinations were made with a protein binding dye, Sulforhodamine B. Results for each compound were reported as a mean graph of the percent growth of the treated cells when compared to the untreated control cells. There after obtaining the results for one dose assay, analysis of historical Development Therapeutics Programme (DTP) was performed and compounds, which satisfied pre-determined threshold inhibition criteria was selected for NCI full panel 5 dose assay. [40-43]

4.1.3 In vitro 5 dose full NCI 60 cell panel assay

All the cell lines (about 60), representing nine tumor subpanels, were incubated at five different concentrations (0.01, 0.1, 1, 10 & 100 μM). The outcomes were used to create log concentration Vs % growth inhibition curves and three response parameters (GI_{50}, TGI and LC_{50}) were calculated for each cell line. The GI_5 value (growth inhibitory activity) corresponds to the concentration of the compound causing 50% decrease in net cell growth, the TGI value (cytostatic activity) is the concentration of the compound resulting in total growth inhibition and LC_{50} value (cytotoxic activity) is the concentration of the compound causing net 50% loss of initial cells at the end of the incubation period of 48 h. [40-43]

4.2 EGFR Kinase Inhibitory assay

The assays were performed in vitro using Homogeneous timeresolved fluorescence (HTRF) method (Cisbio). EGFR and EGFR T790M were purchased from Sigma. The kinases and substrates were incubated first with synthesized analogues for 5 min in enzymatic buffer. Then ATP (Sigma) was added into the reaction mixture to start the enzyme reaction. The ATP concentrations used in each enzyme reaction were 1.65 µM for EGFR, equivalent to the *Km* of ATP for the corresponding enzyme in this assay condition. The assays were conducted at room temperature for 30 min and stopped by detection reagents which contain EDTA. The detection step lasted for 1 h. The IC_{50} was calculated using GraphPad Prism 5.0.[44]

5. Docking Study

Docking study was carried out using a graphical user interface SP-docking mode of program Maestro 8. [45-47] The protein structure of a complex T790M mutatd EGFR was obtained from the RCSB Protein Data Bank (PDB) as entry 2JIU (http://www.rcsb.org/pdb/explore/explore.2jiu). [48] The protein preparation was carried out using 'protein preparation wizard' in Maestro 8.0 in two steps, preparation and refinement. After ensuring chemical correctness, water molecules in the crystal structures were deleted, and hydrogens were added, wherever they were missing. The energy of crystal structure was minimized. [49]

Grids were defined centering them on the ligand in the crystal structure using the default box size. The ligands were developed using maestro build panel and prepared by Ligprep 2.2 module that produces the low energy conformer of ligands using OPLS 2005 force field. [50] The low energy conformation of the ligands was selected and docked into the grid generated from protein structures using standard precision (SP) docking mode. The final evaluation was done with glide score (docking score), and a single best pose is generated as the output for a particular ligand.

6. Results and Discussion

All the compounds were synthesized as depicted in **Scheme 1**. The structures of final compounds (4-105) were characterized based on their physicochemical and spectral (IR, ^{1}H NMR, ^{13}C NMR and MS) analysis. The analytical data of all the newly synthesized compounds along with their anticipated structures are summarized in supporting information.

The tumor growth inhibition properties of the 32 compounds selected among the all synthesized compounds by National Cancer Institute (NCI), USA. Among the selected 32 compounds, 18 were further screened for 5-log dose molar range as they have shown prominent cell growth inhibition at 10^{-5} M concentration.

To assess the potency for EGFR inhibitory activity, selected 18 compounds were tested against gefitinib-resistant NSCLC cell H1975 possessing L858R/T790M mutant and EGFR human epithelial carcinoma cell A431 overexpressing wild-type. The results of in vitro antiproliferation demonstrate that compound **79**, 7-chloro-3-(5-(4-methoxyphenyl)-1,3,4-thiadiazol-2-yl)-2-phenylquinazolin-4(3*H*)-one was found to be the most active compound of the series with IC_{50} value of 0.031 μM, followed by compound **78** having IC_{50} value of 0.129 μM against H1975 NSCLC cell line. Similarly significant results were shown by compound **23** and **51** with IC_{50} value of 0.81 μM and 0.84 μM (**Table 1**).

Since EGFR is expressing in many tissues for normal cellular processes, the potential for the toxicity from EGFR inhibitors is a concern. Therefore, the growth inhibitory of the compounds against cancer cell lines with low level of EGFR expression was evaluated to assess the potential non-specific toxicity. The cancer cell lines A549 express low levels of EGFR (WT EGFR and k-Ras mutation) and therefore are good counter-screen cell lines for EGFR-targeting inhibitors.

Table 1. Antiproliferative activity of compounds against cells harboring a different status of EGFR.

Compound Code	Structure	NCI-H1975 (EGFR L858R/T790M) (IC_{50} μM)	A549/ATCC (WT EGFR) (IC_{50} μM)	HT 29 (Non-Special Gene Type) (IC_{50} μM)	Selectivity Ratio NCI-H1975/A549
15	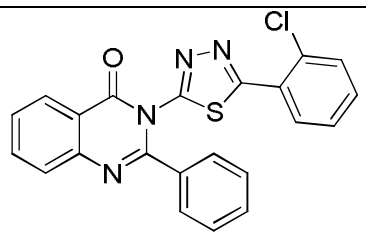	5.23 ± 0.42	100 ± 0.51	32.5 ± 0.13	**0.052**
17	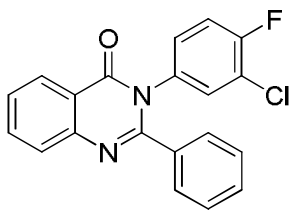	4.89 ± 0.31	5.42 ± 0.23	6.12 ± 0.16	0.90
23	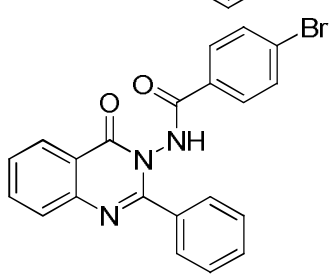	0.81 ± 0.08	0.523 ± 0.05	1.15 ± 0.14	1.54
31	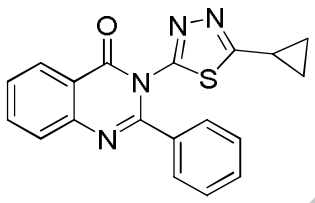	2.38 ± 0.12	3.02 ± 0.34	3.46 ± 0.18	0.78
48	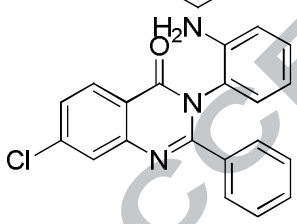	4.87 ± 0.15	18.3 ± 0.45	50 ± 0.32	0.26
51	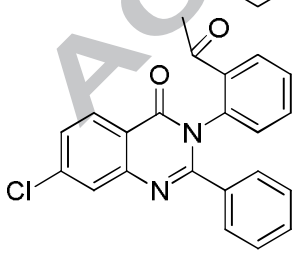	0.846 ± 0.05	50 ± 0.10	50 ± 0.52	**0.016**
55	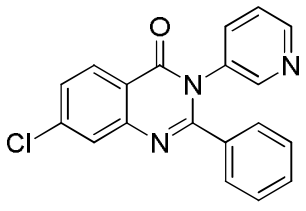	2.45 ± 0.43	3.33 ± 0.23	3.80 ± 0.28	0.73
60	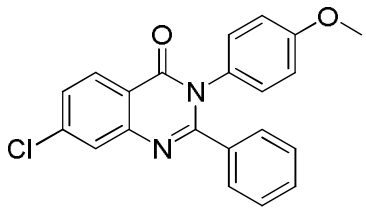	2.88 ± 0.34	2.87 ± 0.34	3.92 ± 0.26	1.00
73	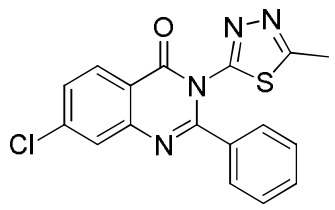	0.76 ± 0.05	3.79 ± 0.11	21.2 ± 0.24	**0.20**
75	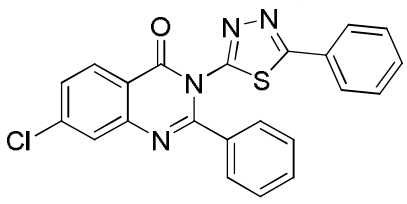	0.213 ± 0.05	2.09 ± 0.33	2.72 ± 0.21	**0.101**
78	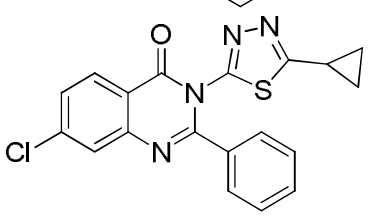	0.129 ± 0.05	0.717 ± 0.05	0.732 ± 0.06	**0.17**

Table 1. Continue...

Compound Code	Structure	NCI-H1975 (EGFR L858R/T790M) (IC_{50} µM)	A549/ATCC (WT EGFR) (IC_{50} µM)	HT 29 (Non-Special Gene Type) (IC_{50} µM)	Selectivity Ratio NCI-H1975/A549
79	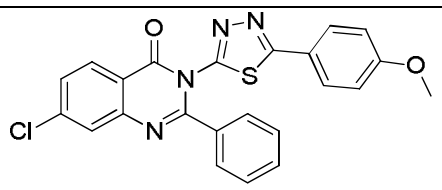	0.031 ± 0.02	0.390 ± 0.05	0.388 ± 0.04	**0.079**
86	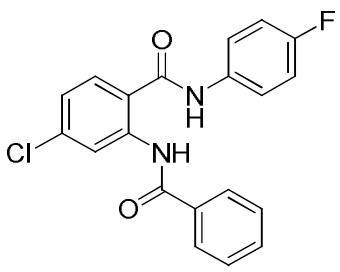	14.41 ± 0.34	17.4 ± 0.28	3.36 ± 0.21	0.82
93	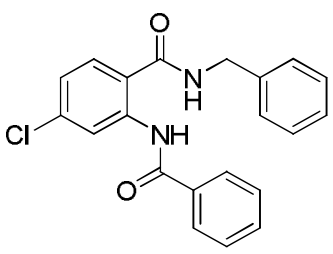	1.67 ± 0.07	1.57 ± 0.08	4.80 ± 0.24	1.06
94	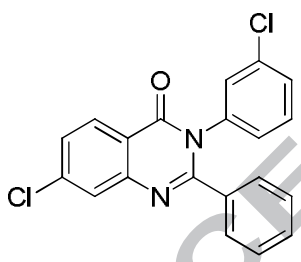	2.45 ± 0.12	5.30 ± 0.28	4.50 ± 0.32	0.46
96	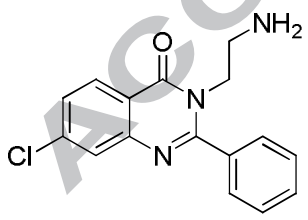	0.378 ± 0.05	2.45 ± 0.10	0.428 ± 0.08	**0.154**
Gefitinib		8.71 ± 0.22	9.86 ± 0.18	8.19 ± 0.32	**0.88**
WZ4002		0.058 ± 0.01	1.87 ± 0.08	2.95 ± 0.08	**0.031**

* Lesser the selectivity ratio towards zero more is selectivity (safety Index)

Table 2. Selectivity profile of **compound 79** against panel of kinases

Kinase	% inhibition at 3 μM
EGFR	78
VEGFR-1	34
VEGFR-2	42
Abl	0
AMPKα1	0
urora-1	0
Blk	0
CDK1	0
cKIT	0
FAK	0
FGFR1	0
Flt1	0
Flt3	0
IGF-1R	10
IR	0
JAK-2	0
LKB-1	0
MEK-1	0
Met	0
Syk	0

This test was conducted by Millipore Kinase Profiling Service.

Table 3. *In vitro* inhibition of EGFR tyrosine kinase activity

Compound	Structure	EGFR Inhibition IC_{50} (µM)	
		T790M EGFR	**WT EGFR**
15	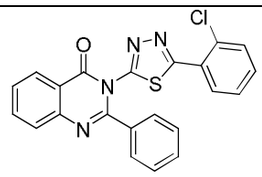	7.23 ± 0.10	78.23 ± 0.12
23	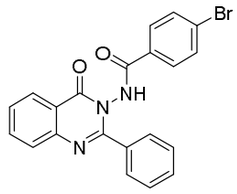	0.78 ± 0.05	0.42 ± 0.02
51	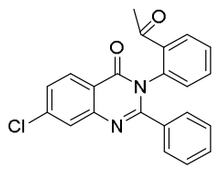	0.72 ± 0.05	34.32 ± 0.21
73	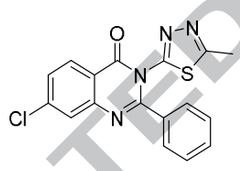	12.12 ±0.10	3.21 ± 0.21
75	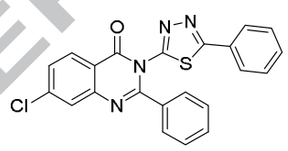	1.12 ± 0.08	1.68 ± 0.09
78	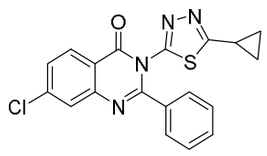	0.102 ± 0.01	0.53 ± 0.01
79	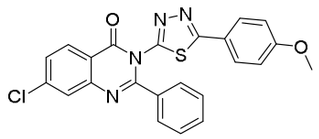	0.021 ± 0.001	0.32 ± 0.02
96	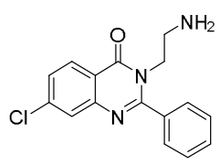	0.287 ± 0.05	2.11 ± 0.08
Gefitinib		0.173 ± 0.06	0.076 ± 0.001

EGFR activity assays were performed using HTRF method. The data reported are the mean values from three independent experiments

These compounds are also evaluated against HT-29 colon cancer cells, which expressed a non-special gene type, to test their toxic effects. As shown in **Table 1** compounds **15**, **51**, **73**, **75**, **78**, **79** and **96** were less potent against A549 (WT EGFR and k-Ras mutation) and HT-29 (non-special gene type) cells, showing a high safety index. Therefore, compounds **15**, **51**, **73**, **75**, **78**, **79** and **96** might be promising candidates to overcome drug resistance mediated by the EGFR T790Mutant.

The inhibitory activity of 79 against various kinases is summarized in **Table 2** and results confirmed that 79 is a selective EGFR inhibitor. The inhibitory activities of the selected compounds against different types of kinases (EGFR T790M, EGFR WT) were evaluated using Homogeneous time-resolved fluorescence (HTRF) method, and gefitinib was employed as positive controls. Notably compound **79** and **78** shows significant T790M inhibitory activity of IC_{50} value 0.021 μM and 0.102 μM. Inhibition of WT EGFR leads to the dose-limiting toxicity such as diarrhoea and skin rash. Therefore, the clinical application of these inhibitors has been limited, especially in patients with gefitinib or erlotinib-resistant NSCLC. As shown in **Table 3**, all the tested compounds displayed weaker inhibitory WT EGFR. The results indicate that the non-specific cytotoxic effects of this hybrid are minimal

Lung cancers caused by activating mutations in the epidermal growth factor receptor (EGFR) are initially responsive to small molecule tyrosine kinase inhibitors (TKIs), but the efficacy of these agents is often limited because of the emergence of drug resistance conferred by a second mutation, T790M. Threonine 790 is the ‘‘gatekeeper’’ residue, an important determinant of inhibitor specificity in the ATP binding pocket. The T790M mutation has been thought to cause resistance by sterically blocking binding of TKIs such as gefitinib and erlotinib.

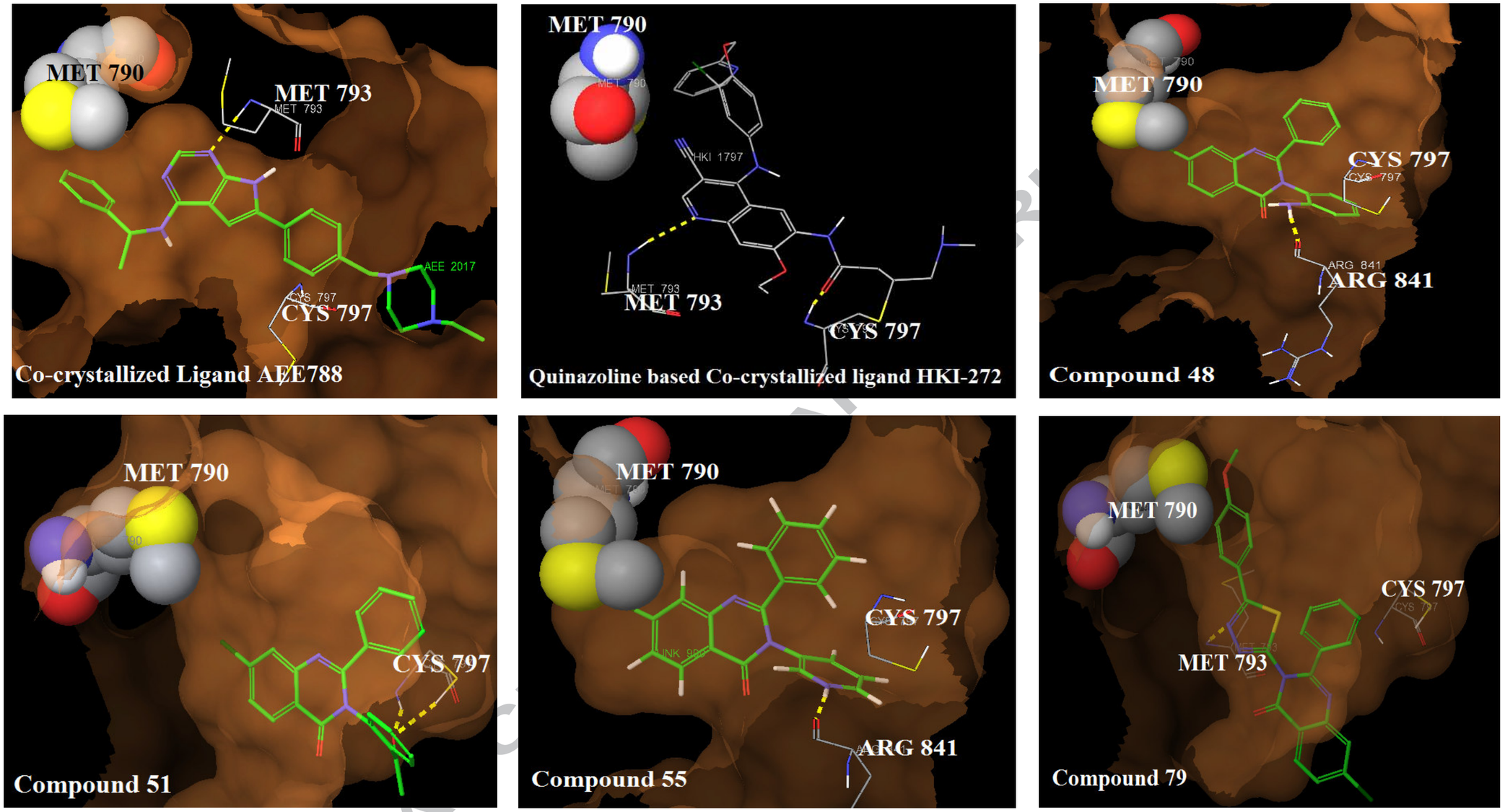

Fig. 3a. Docking interaction of the active compounds with T790M EGFR-tyrosine kinase PDB: 2JIU.

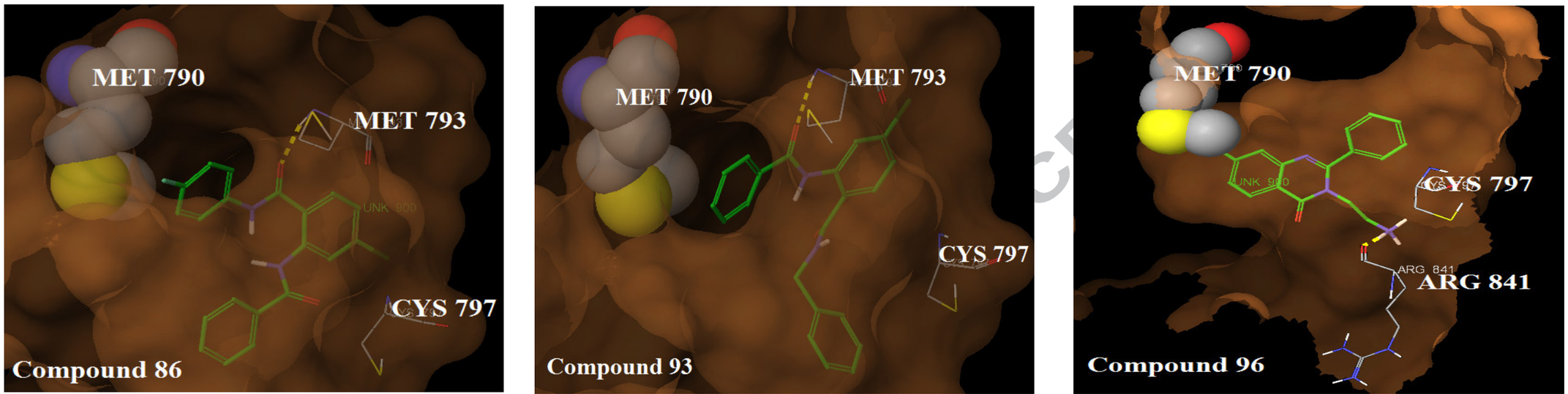

Fig. 3b. Docking interaction of the active compounds with T790M EGFR-tyrosine kinase PDB: 2JIU.

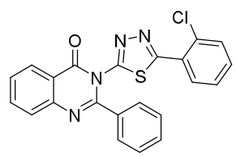

IC_{50}= 5.23 µM

NSC:99068/755727
Compound No. 15

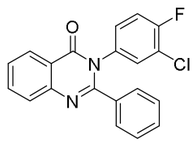

IC_{50}= 4.89 µM

NSC: 100065/754909
Compound No. 17

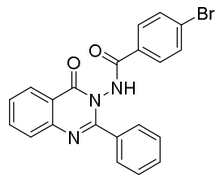

IC_{50}= 0.81 µM

NSC: 95678/755724
Compound No. 23

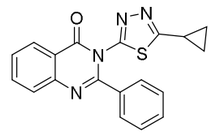

IC_{50}= 2.38 µM

NSC: 100250/754910
Compound No. 31

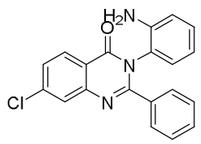

IC_{50}= 4.87 µM

NSC: 95675/755723
Compound No. 48

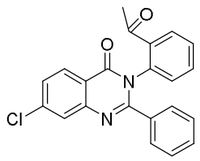

IC_{50}= 0.846 µM

NSC: 101783/755741
Compound No. 51

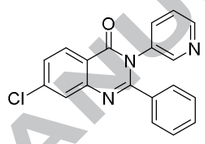

IC_{50}= 2.45 µM

NSC: 101786/755744
Compound No. 55

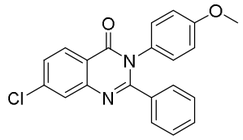

IC_{50}= 2.88 µM

NSC: 100552/755739
Compound No. 60

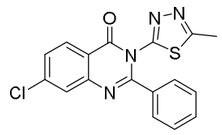

IC_{50}= 0.76 µM

NSC: 107576/760523
Compound No. 73

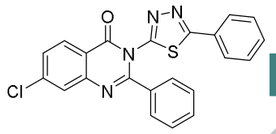

IC_{50}= 0.213 µM

NSC: 107891/760526
Compound No. 75

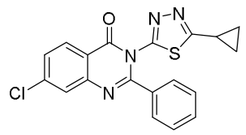

IC_{50}= 0.129 µM

NSC: 107894/760527
Compound No. 78

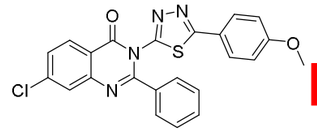

IC_{50}= 0.031 µM

NSC: 107896/760528
Compound No. 79

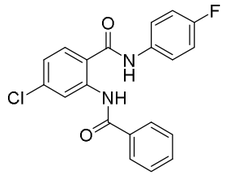

IC_{50}= 14.41 µM

NSC: 100527/755734
Compound No. 86

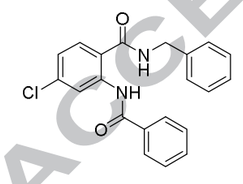

IC_{50}= 1.67 µM

NSC: 100546/755735
Compound No. 93

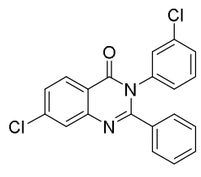

IC_{50}= 2.45 µM

NSC: 100547/755736
Compound No. 94

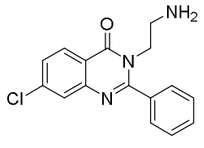

IC_{50}= 0.378 µM

NSC: 102283/756960
Compound No. 96

Fig. 4. Structure activity relationship (**NCI-H1975**)

Docking studies revealed that the synthesized compounds binds differently to the ATP-binding site of the T790M EGFR tyrosine kinase domain as compare to the existing first, second and third generation agent. The compounds having hydrogen bond donor at 3rd position of quinazoline show hydrogen bond interaction with the Arg 841 amino acid of T790M EGFR rather than interacting with Met793 (compounds **48**,**55** and **96**) as shown in **Fig. 3a** and **3b**. Such kind of allosteric site binding of the compounds to the T790M EGFR could resolve the problem of resistance. Since the predominant strategy to combat the resistance is the use of covalent inhibitors, increasing target residence time and providing strong potency. For this reason, second and third generation EGFR inhibitors have been designed to form a covalent bond with Cys797 showing promising efficacy. On the other hands thiadiazoles (C-3 position of quinazoline) and ring open quinazolines interact *via* Met-793 reversibly except compound **51**, which shows reversible hydrogen bonding interaction with that of Cys-797 as shown in **Fig. 3a** and **3b**. These findings indicate that drugs owning excellent potency on EGFR without relying on the covalent modification of C797 are in demand. Herein, our work indicates alternative noncovalent strategy that provides new inhibitors with the potency to overcome the problem of gefitinib-resistance. It will also provide chemical starting points for optimization of the efficacy/toxicity ratio.

7. Structure Activity Relationship

Structure-activity correlation of the synthesized compounds against NCI-H1975 revealed that, quinazolines having chloro substituent at 7th position; is more active as compared to the unsubstituted quinazoline derivatives (compound **78** and **31**), which could contribute in enhancement of lipid solubility compounds. Presence of bulkier group at 3rd position of the quinazolines gave significant results. It is also observed that ring opened quinazolines (diamides) are not as active as that of the ring closed quinazolines (compound **86** and **93**) and confirms that

the quinazoline ring is satisfactory backbone for anti-tumor activity. 2-amino-1,3,4-thiadiazoles having chloro substitution at 7th position are more potent as compared to the anilines at third position of quinazolines. 4-methoxy phenyl is more potent on 1,3,4-thiadiazoles as compare to the other substitution (compound **79**). Compound **15** containing 4-chlorophenyl on 1,3,4-thiadiazoles was less potent against A549 (WT EGFR and k-Ras mutation) and HT-29 (non-special gene type) cells, showing a high safety index. It could be crucial chemical starting points for the optimization of the efficacy/toxicity ratio, which is major problem of second and third generation EGFR inhibitors. Among the anilines at 3rd position of quinazolines; 3-chloro 4-fluro aniline has come out with significant results as compared to other anilines (compounds **17**) (**Fig. 4**).

8. Conclusion

New derivatives of 4(3*H*)-quinazolinones were synthesized and evaluated for their inhibitory activity against NSCLC (Non Small Cell Lung Cancer cell lines). The results of the study demonstrated that compound **79**, 7-chloro-3-(5-(4-methoxyphenyl)-1,3,4-thiadiazol-2-yl)-2-phenylquinazolin-4(3*H*)-one was found to be the most potent compounds of the series with IC_{50} value of 0.031 μM. Compounds **15**, **51**, **73**, **75**, **78**, **79** and **96** were less potent against **A549** (WT EGFR and k-Ras mutation) and HT-29 (non-special gene type) cells, showing a high safety index. The obtained results showed that compounds **15**, **48**, **51**, **78**, **86** could be useful as a template for future design, optimization, and investigation to construct more active analogs to overcome drug resistance mediated by the EGFR T790M mutant. The inhibitory effect of selected potent compounds on T790M EGFR tyrosine kinase activity was determined and Compound **78** (0.102 μM) and 79 (0.021 μM) exhibited significant inhibition with subnanomolar IC_{50} values as compare to the gefitinib. Docking studies further revealed that the quinazolinones

(**48**, **55** and **96**) allosterically binds to the Arg 841 amino acid of T790M EGFR rather than interacting with Met793 *via* substitution at 3rd position of quinazoline. Herein, our work indicates alternative noncovalent strategy that provides new inhibitors with the potency to overcome the problem of gefitinib-resistance. It will also provide chemical starting points for optimization of the efficacy/toxicity ratio. Structure-activity correlation of the synthesized compounds revealed that, quinazolines having chloro substituent at 7th position is more active as compared to the unsubstituted quinazoline derivatives. Presence of bulkier group at 3rd position of the quinazolines gave significant results. Finally, it is conceivable that further derivatization of such compounds will be of interest with the hope to get more selective and potent T790M EGFR inhibitors, which could overcome EGFR resistance obstacle.

9. Experimental [39]

All the chemicals and solvents were supplied by Sigma-Aldrich and Spectrochem Pvt Ltd. Solvents were distilled and dried before use if required. The reactions were monitored with the help of thin-layer chromatography using pre-coated aluminum sheets with GF_{254} silica gel, 0.2 mm layer thickness (Merck) and the solvent systems of Benzene : Acetone (7:3 and 9:1), Toluene: Ethyl acetate: Formic acid (5:4:1) and Chloroform: Methanol (9:1) were used. The spots were visualized under UV lamp. Melting points of the synthesized compounds were determined using one end open capillary tubes on a liquid paraffin bath and are uncorrected. IR spectrum was acquired on Perkin Elmer FT-IR spectrometer. Both ^{1}H-NMR (DMSO) and ^{13}C NMR (DMSO) spectra of the synthesized compounds were performed with Bruker Avance-II 400 NMR Spectrometer operating at 400 MHz and 100 MHz respectively in SAIF, Punjab University (Chandigarh) and the chemical shifts are reported in ppm units with respect to TMS

as internal standard. Mass spectra of the synthesized compounds were recorded at MAT 120 in SAIF, Punjab University.

9.1 2-phenyl-4H-benzo[d][1,3]oxazin-4-one (3a and 3b)

It is synthesized as per the reported method.[39]

9.2 General procedure for the synthesis of title compounds 3-substituted-2-phenylquinazolin-4(3H)-ones

Equimolar quantity of 2-phenyl-4*H*-benzo[*d*][1,3]oxazin-4-one **3a** or 7-chloro-2-phenyl-4*H*-benzo[*d*][1,3]oxazin-4-one **3b** and different primary amino group containing moieties were fused together at 200-250 °C in an oil bath for 30 minutes, in such way that reaction mixture should not degraded due to high heating. The mixture was cooled and ethanol was added to the mixture. The separated solid was collected by filtration, washed with ethanol, dried and recrystallized multiple times with ethanol to get the pure product.

9.2.1 3-(5-(2-chlorophenyl)-1,3,4-thiadiazol-2-yl)-2-phenylquinazolin-4(3H)-one (15)

Yield 69 %; mp above 250 °C; IR (KBr) ν_{max} 3098.12 (Arom.CH strech), 2918.68 (Aliph.CH strech), 1671.12 (C=O), 1561.11 (C=C), 1465.48 (CH bend), 731.12 (C-Cl) cm^{-1}; ^{1}H NMR (DMSO-d_6) δ 7.11-8.14 (m, 12H, Ar-H), 2.45 (s, 3H, CH_3); ^{13}C NMR (DMSO-d_6) δ 175.14, 170.15, 164.18, 158.28, 150.15, 140.16, 135.67, 134.16, 132.89, 132.67, 131.65, 130.86, 129.68, 128.50, 128.00, 127.66, 127.00, 126.86, 126.00, 122.14, 24.36. HRMS (ESI) m/z calcd. for $C_{22}H_{13}ClN_4OS$: 416.0499; found: 416.0492.

9.2.2 3-(3-chloro-4-fluorophenyl)-2-phenylquinazolin-4(3H)-one (17)

Yield 68 %; mp 168-170 °C; IR (KBr) ν_{max} 3060.36 (CH strech), 1680.53 (C=O), 1604.96 (C=C), 1445.27 (CH bend), 1084.23 (C-F), 770.71 (C-Cl) cm^{-1}; ^{1}H NMR (DMSO-d_6) δ 6.92-8.23 (m, 12H, Ar-H); ^{13}C NMR (DMSO-d_6) δ 162.06, 158.88, 156.38, 154.59, 134.92, 134.09,

134.05, 131.52, 129.15, 129.08, 128.88, 128.35, 127.86, 127.69, 121.65, 120.64, 116.92; HRMS (ESI) m/z calcd. for $C_{20}H_{12}ClFN_2O$: 350.0622; found: 350.0629.

9.2.3 4-bromo-N-(4-oxo-2-phenylquinazolin-3(4H)-yl) benzamide (23)

Yield 41 %; mp 221-224 $^{\circ}$C; IR (KBr) ν_{max} 3282.34 (NH strech), 3083.26 (CH strech), 1728.72 [C=O (ketone)], 1672.38 [C=O (amide)], 1626.84 (NH bend), 1568.26 (C=C), 1452.97 (CH bend), 601.83 (C-Br) cm^{-1}; ^{1}H NMR (DMSO-d_6) δ 11.31 (s, 1H, NH), 6.82-7.98 (m, 13H, Ar-H); ^{13}C NMR (DMSO-d_6) δ 166.37, 162.15, 158.36, 152.32, 135.98, 132.84, 131.86, 130.68, 129.65, 128.94, 128.47, 128.00, 127.80, 126.5, 126.37, 126.00, 120.90. HRMS (ESI) m/z calcd. for $C_{21}H_{14}BrN_3O_2$: 419.0269; found: 419.0274.

9.2.4 3-(5-cyclopropyl-1,3,4-thiadiazol-2-yl)-2-phenylquinazolin-4(3H)-one (31)

Yield 81 %; mp 224-228 $^{\circ}$C; IR (KBr) ν_{max} 3068.74 (Arom.CH strech), 2973.01 (Aliph.CH strech), 1677.32 (C=O), 1560.25 (C=C), 1468.23 (CH bend) cm^{-1}; ^{1}H NMR (DMSO-d_6) δ 7.17-8.88 (m, 9H, Ar-H), 1.08-2.34 (m, 5H, cyclopropyl); ^{13}C NMR (DMSO-d_6) δ 175.41, 170.90, 159.15, 146.90, 140.84, 134.81, 134.45, 131.99, 129.45, 128.83, 127.42, 123.22, 121.44, 117.58, 11.09, 10.65; HRMS (ESI) m/z calcd. for $C_{19}H_{14}N_4OS$: 347.0888; found: 347.0882 [M+1].

9.2.5 3-(2-aminophenyl)-7-chloro-2-phenylquinazolin-4(3H)-one (48)

Yield 62 %; mp above 250 $^{\circ}$C; IR (KBr) ν_{max} 3171.26 and 3131.98 (NH_2), 3065.33 (CH strech), 1671.48 (C=O), 1602.48 (NH bend), 1569.04 (C=C), 1444.24 (CH bend), 693.14 (C-Cl) cm^{-1}; ^{1}H NMR (DMSO-d_6) δ 7.14-8.21 (m, 12H, Ar-H), 6.65 (s, 2H, NH_2); ^{13}C NMR (DMSO-d_6) δ 161.67, 151.26, 149.21, 143.67, 134.91, 130.08, 129.49, 128.55, 126.35, 122.27, 121.47, 121.23, 118.63, 118.09, 114.92, 114.64, 111.08, 110.55; HRMS (ESI) m/z calcd. for $C_{20}H_{14}ClN_3O$: 348.0825; found: 348.0831 [M+1].

9.2.6 3-(2-acetylphenyl)-7-chloro-2-phenylquinazolin-4(3H)-one (51)

Yield 32 %; mp 192-194 °C; IR (KBr) ν_{max} 3111.20 (Arom.CH strech), 2924.66 (Aliph.CH strech), 1681.55 [C=O (ketone)], 1645.32 [C=O (amide)], 1606.71 (C=C), 1421.30 (CH bend), 759.92 (C-Cl) cm^{-1}; ^1H NMR (DMSO-d_6) δ 7.23-8.38 (m, 12H, Ar-H), 2.74 (s, 3H, CH_3); ^{13}C NMR (DMSO-d_6) δ 199.14, 164.94, 160.01, 141.35, 139.60, 138.65, 134.81, 133.88, 131.72, 131.66, 128.39, 128.33, 126.82, 123.09, 122.79, 122.03, 120.58, 120.47, 118.13, 28.16; HRMS (ESI) m/z calcd. for $C_{22}H_{15}ClN_2O_2$: 375.0822; found: 375.0828[M+1].

9.2.7 7-chloro-2-phenyl-3-(pyridin-3-yl) quinazolin-4(3H)-one (55)

Yield 81 %; mp 230-235 °C; IR (KBr) ν_{max} 3063.52 (CH strech), 1684.71 (C=O), 1598.68 (C=C), 1421.88 (CH bend), 702.79 (C-Cl) cm^{-1}; ^1H NMR (DMSO-d_6) δ 7.25-8.50 (m, 12H, Ar-H); ^{13}C NMR (DMSO-d_6) δ 161.49, 155.82, 149.65, 149.34, 148.30, 141.35, 136.48, 134.42, 134.34, 130.01, 129.07, 128.67, 128.44, 128.21, 127.49, 123.51, 119.06; HRMS (ESI) m/z calcd. for $C_{19}H_{12}ClN_3O$: 334.0669; found: 334.0671[M+1].

9.2.8 7-chloro-3-(4-methoxyphenyl)-2-phenylquinazolin-4(3H)-one (60)

Yield 62 %; mp 200-204 °C; IR (KBr) ν_{max} 3056.62 (CH strech), 1711.81 (C=O), 1595.94 (C=C), 1446.28 (CH bend), 771.14 (C-Cl) cm^{-1}; ^1H NMR (DMSO-d_6) δ 6.68-7.52 (m, 12H, Ar-H), 3.78 (s, 3H, OCH_3); ^{13}C NMR (DMSO-d_6) δ 65.89, 160.23, 156.12, 150.04, 138.41, 134.13, 132.29, 130.12, 129.94, 128.92, 127.95, 127.46, 123.05, 121.70, 119.34, 113.16, 55.44; HRMS (ESI) m/z calcd. for $C_{21}H_{15}ClN_2O_2$: 363.0822; found: 363.0825 [M+1].

9.2.9 7-chloro-3-(5-methyl-1,3,4-thiadiazol-2-yl)-2-phenylquinazolin-4(3H)-one (73)

Yield 68 %; mp 243-247 °C; IR (KBr) ν_{max} 3064.98 (Arom.CH strech), 2923.34 (Aliph.CH strech), 1686.93 (C=O), 1590.32 (C=C), 1462.36 (CH bend), 724.38 (C-Cl) cm^{-1}; ^1H NMR (DMSO-d_6) δ 6.74-7.81 (m, 8H, Ar-H), 2.81 (s, 3H, CH_3); ^{13}C NMR (DMSO-d_6) δ 171.31,

163.43, 158.44, 154.35, 146.32, 138.43, 132.62, 130.65, 129.62, 129.20, 129.01, 128.60, 124.62, 120.33, 22.30. HRMS (ESI) m/z calcd. for $C_{17}H_{11}ClN_4OS$: 354.0342; found: 354.0347.

9.7.10 7-chloro-2-phenyl-3-(5-phenyl-1,3,4-thiadiazol-2-yl)quinazolin-4(3H)-one (75)

Yield 45 %; mp above 250 °C; IR (KBr) ν_{max} 3023.98 (CH strech), 1668.84 (C=O), 1568.47 (C=C), 1472.62 (CH bend), 710.23 (C-Cl) cm^{-1}; ^1H NMR (DMSO-d_6) δ 6.89-8.34 (m, 13H, Ar-H); ^{13}C NMR (DMSO-d_6) δ 172.35, 170.14, 162.34, 158.35, 156.35, 139.43, 135.65, 132.64, 132.15, 130.25, 129.63, 128.62, 128.43, 126.45, 126.14, 124.35, 122.34, 120.35. HRMS (ESI) m/z calcd. for $C_{22}H_{13}ClN_4OS$: 416.0499; found: 416.0493.

9.2.11 7-chloro-3-(5-cyclopropyl-1,3,4-thiadiazol-2-yl)-2-phenylquinazolin-4(3H)-one (78)

Yield 68 %; mp 222-226 °C; IR (KBr) ν_{max} 3123.35 (Arom.CH strech), 2956.32 (Aliph.CH strech), 1665.87 (C=O), 1543.76 (C=C), 1446.87 (CH bend), 678.92 (C-Cl) cm^{-1}; ^1H NMR (DMSO-d_6) δ 7.31-8.21 (m, 8H, Ar-H), 1.10-2.61 (m, 5H, cyclopropyl); ^{13}C NMR (DMSO-d_6) δ 171.36, 166.37, 162.35, 158.37, 154.48, 139.45, 132.66, 132.37, 130.89, 130.67, 130.25, 128.65, 124.66, 120.37, 11.25, 10.86. HRMS (ESI) m/z calcd. for $C_{19}H_{13}ClN_4OS$: 380.0499; found: 380.0493.

9.2.12 7-chloro-3-(5-(4-methoxyphenyl)-1,3,4-thiadiazol-2-yl)-2-phenylquinazolin-4(3H)-one (79)

Yield 63 %; mp above 250 °C; IR (KBr) ν_{max} 3046.38 (CH strech), 1658.24 (C=O), 1572.82 (C=C), 1462.83 (CH bend), 756.32 (C-Cl) cm^{-1}; ^1H NMR (DMSO-d_6) δ 6.81-8.12 (m, 12H, Ar-H), 3.85 (s, 3H, OCH_3); ^{13}C NMR (DMSO-d_6) δ 172.67, 169.45, 162.36, 160.37, 158.85, 156.36,

139.47, 132.66, 132.17, 130.67, 130.35, 128.52, 128.40, 127.64, 126.35, 124.68, 120.66, 118.33, 55.67. HRMS (ESI) m/z calcd. for $C_{23}H_{15}ClN_4O_2S$: 446.0604; found: 446.0609.

9.2.13 2-benzamido-4-chloro-N-(4-fluorophenyl) benzamide (86)

Yield 73 %; mp 245-248 °C; IR (KBr) ν_{max} 3264.62 (NH strech), 3150.42 (CH strech), 1651.20 (C=O), 1601.11 (NH bend), 1550.26 (C=C), 1408.83 (C-H bend), 1223.84 (C-F), 702.43 (C-Cl) cm^{-1}; ^1H NMR (DMSO-d_6) δ 12.03 (s, 1H, NHCO), 10.71(s, 1H, CONH), 6.83-8.69 (m, 12H, Ar-H); ^{13}C NMR (DMSO-d_6) δ 166.76, 164.01, 159.28, 140.56, 139.04, 134.03, 132.41, 128.97, 128.08, 127.42, 123.07, 122.79, 122.71, 121.67, 119.28, 116.04, 115.82; HRMS (ESI) m/z calcd. for $C_{20}H_{14}ClFN_2O_2$: 391.0728; found: 391.0735 [M+Na].

9.2.14 2-benzamido-N-benzyl-4-chlorobenzamide (93)

Yield 68 %; mp 200-205 °C; IR (KBr) ν_{max} 3257.31 (NH strech), 3111.10 (CH strech), 1652.02 (C=O), 1600.85 (NH bend), 1561.87 (C=C), 1413.34 (C-H bend), 705.37 (C-Cl) cm^{-1}; ^1H NMR (DMSO-d_6) δ 11.57 (s, 1H, NHCO), 10.14 (s, 1H, CONH), 6.91-8.84 ((m, 13H, Ar-H), 4.63 (s, 2H, CH_2); ^{13}C NMR (DMSO-d_6) δ 167.43, 165.78, 140.93, 138.81, 137.36, 134.30, 132.19, 128.92, 128.89, 127.87, 127.80, 127.42, 122.86, 121.33, 118.37, 44.16; HRMS (ESI) m/z calcd. for $C_{21}H_{17}ClN_2O_2$: 364.0979; found: 364.0973.

9.2.15 7-chloro-3-(3-chlorophenyl)-2-phenylquinazolin-4(3H)-one (94)

Yield 71 %; mp 194-200 °C; IR (KBr) ν_{max} 3069.99 (CH strech), 1686.80 (C=O), 1580.47 (C=C), 1447.27 (CH bend), 701.77 (C-Cl) cm^{-1}; ^1H NMR (DMSO-d_6) δ 6.77-8.70 (m, 12H, Ar-H); ^{13}C NMR (DMSO-d_6) δ 161.48, 155.96, 141.21, 138.41, 134.67, 134.65, 129.94, 129.88,

129.42, 128.97, 128.93, 128.89, 128.67, 128.26, 128.10, 127.41, 127.38, 119.20; HRMS (ESI) m/z calcd. for $C_{20}H_{12}Cl_2N_2O$: 367.0327; found: 367.0321 [M+1].

9.2.16 3-(2-aminoethyl)-7-chloro-2-phenylquinazolin-4(3H)-one (96)

Yield 89 %; mp 223-228 $^{\circ}$C; IR (KBr) ν_{max} 3268.12 and 3214.78 (NH_2), 3087.21 (Arom.CH strech), 2912.98 (Aliph.CH strech), 1656.12 (C=O), 1601.78 (NH bend), 1491.23 (C=C), 1438.12 (CH bend), 712.98 (C-Cl) cm^{-1}; ^{1}H NMR (DMSO-d_6) δ 6.98-7.97 (m, 8H, Ar-H), 6.11 (s, 2H, NH_2,), 2.91 (t, 2H, CH_2); ^{13}C NMR (DMSO-d_6) δ 160.11, 158.25, 154.34, 139.30, 132.26, 132.05, 130.87, 130.24, 130.00, 129.45, 124.84, 120.87, 50.14, 36.39. HRMS (ESI) m/z calcd. for $C_{16}H_{14}ClN_3O$: 299.0825; found: 299.0829.

Acknowledgement

The authors would like to thank "Science and Engineering Research Board (SERB) of Department of Science and Technology (DST) Govt. of India" (Grant No.YSS/2015/002017) for funding the project.

REFERENCES

1. Ohashi, K.; Maruvka, Y.E.; Michor, F.; Pao, W. *J. Clin. Oncol.* **2013**, 31,1070−1080.
2. Siegel, R.; Naishadham, D.; Jemal A. *Cancer J. Clin.* **2012**, 62, 10−29.
3. Sequist, L.V.; Martins, R.G.; Spigel, D.; Grunberg, S.M.; Spira, A.; Jänne, P.A.; Joshi, V.A.; McCollum, D.; Evans, T.L.; Muzikansky, A.; Kuhlmann, G.L.; Han, M.; Goldberg, J.S.; Settleman, J.; Iafrate, A.J.; Engelman, J.A.; Haber, D.A.; Johnson, B.E.; Lynch, T.J. *J. Clin. Oncol.* **2008**, 26, 2442−2449.
4. Sharma, S.V.; Bell, D.W.; Settleman, J.; Haber, D.A. *Nat. Rev. Cancer.* **2007**, 7, 169−181.
5. Johnson, J.R.; Cohen, M.; Sridhara, R.; Chen, Y.F.; Duan, J.; Gobburu, J.; Booth, B.; Benson, K.; Leighton, J.; Hsieh, L.S.; Chidambaram, N.; Zimmerman, P.; Pazdur, R. *Clin. Cancer Res.* **2005**, 11, 6414−6421.
6. Han, S.W.; Kim, T.Y.; Hwang, P.G.; Jeong, S.; Kim, J.; Choi, I.S.; Oh, D.Y.; Kim, J.H.; Kim, D.W.; Chung, D.H.; Im, S.A.; Kim, Y.T.; Lee, J.S.; Heo, D.S.; Bang, Y.J.; Kim, N. K. *J. Clin. Oncol.* **2005**, 23, 2493−2501.
7. Greulich, H.; Chen, T.H.; Feng, W.; Jänne, P.A.; Alvarez, J.V.; Zappaterra, M.; Bulmer, S.E.; Frank, D.A.; Hahn, W.C.; Meyerson, W.R.M. *PLoS Med.* **2005**, 2, e313.
8. Yang, J.; Wang, W.; Liu, J. J. *J. Med. Chem.* **2012**, 55, 10685-10699.
9. Ladanyi, M.; Pao, W. *Mod. Pathol.* **2008**, 21, S16-22.
10. Pao, W.; Miller, V.A.; Politi, K.A.; Riely, G. J.; Somwar, R.; Zakowski, M.F.; Kris, M.G.; Varmus, H. *PLoS Med.* **2005**, 2, e73.
11. Kobayashi, S.; Boggon, T.J.; Dayaram, T.; Janne, P.A.; Kocher, O.; Meyerson, M.; Johnson, B.E.; Eck, M.J.; Tenen, D.G.; Halmos, B. *New Engl. J. Med.* **2005**, 352,786-792.

12. Yun, C.H.; Mengwasser, K. E.; Toms, A. V.; Woo, M. S.; Greulich, H.; Wong, K. K.; Meyerson, M.; Eck, M. J. *Proc. Natl. Acad. Sci. USA*. **2008**, 105, 2070-2075.

13. Janne, P. A.; von Pawel, J.; Cohen, R. B.; Crino, L.; Butts, C. A.; Olson, S. S.; Eiseman, I. A.; Chiappori, A. A.; Yeap, B. Y.; Lenehan, P. F.; Dasse, K.; Sheeran, M.; Bonomi, P. D. *J. Clin. Oncol.***2007**, 25, 3936-3944.

14. Murakami, H.; Tamura, T.; Takahashi, T.; Nokihara, H.; Naito, T.; Nakamura, Y.; Nishio, K.; Seki, Y.; Sarashina, A.; Shahidi, M.; Yamamoto, N. *Cancer Chemoth. Pharm.* **2012**, 69, 891-899.

15. Sequist, L. V.; Besse, B.; Lynch, T. J.; Miller, V. A.; Wong, K. K.; Gitlitz, B.; Eaton, K.; Zacharchuk, C.; Freyman, A.; Powell, C.; Ananthakrishnan, R.; Quinn, S.; Soria, J. C. *J. Clin. Oncol.* **2010**, 28, 3076-3083.

16. Ramalingam, S. S.; Blackhall, F.; Krzakowski, M.; Barrios, C. H.; Park, K.; Bover, I.; Seog Heo, D.; Rosell, R.; Talbot, D. C.; Frank, R.; Ruiz-Garcia, S. P. A.; Taylor, I.; Liang, J. Q.; Campbell, A. K.; O'Connell, J.; Boyer, M. *J. Clin. Oncol.* **2012**, 30, 3337-3344.

17. Riely, G. J. *J. Thorac. Oncol.* **2008**, 3, S146-149.

18. Eck, M. J.; Yun, C. H. *Biochim. Biophys. Acta.* **2010**, 1804, 559–566.

19. Mishani, E.; Abourbeh, G.; Jacobson, O.; Dissoki, S.; Ben Daniel, R.; Rozen, Y.; Shaul, M.; Levitzki, M. *J. Med. Chem.* **2005**, 48, 5337–5348.

20. Chang, S.; Zhang, L.; Xu, S.; Luo, J.; Lu, X.; Zhang, Z.; Xu, T.; Liu, Y.; Tu, Z.; Xu, Y.; Ren, X.; Geng, M.; Ding, J.; Pei, D.; Ding, K. *J. Med. Chem.* **2012**, 55, 2711–2723.

21. Zhou, W. J.; Ercan, D.; Chen, L.; Yun, C. H.; Li D.; Capelletti, M.; Cortot, A. B.; Chirieac, L.; Iacob, R. E.; Padera, R.; Engen, J. R.; Wong, K. K.; Eck, M. J.; Gray, N. S.; Jänne, P. A. *Nature*. **2009**, 462, 1070–1074.

22. Kwak, E.L.; Sordella, R.; Bell, D. W.; Godin, H. N.; Okimoto, R. A.; Brannigan, B. W.; Harris, P. L.; Driscoll, D. R.; Fidias, P.; Lynch, T. J.; Rabindran, S. K.; McGinnis, J. P.; Wissner, A.; Sharma, S. V.; Isselbacher, K. J.; Settleman, J.; Haber, D. A. *Proc. Natl. Acad. Sci. U.S.A.* 2005,**102**, 7665–7670.

23. Belani, C. P. *Cancer Invest.* **2010**, 28, 413–423.

24. Wong, K. K. *Clin. Cancer Res.* **2007**,13, 4593–4596.

25. Erlichman, C.; Hidalgo, M.; Boni, J. P.; Martins, P.; Quinn, S. E.; Zacharchuk, C.; Amorusi, P.; Adjei, A. A.; Rowinsky, E. K. *J. Clin. Oncol.* **2006**, 24, 2252–2260.

26. Li, D.; Ambrogio, L.; Shimamura, T.; Kubo, S.; Takahashi, M.; Chirieac, L. R.; Padera, R. F.; Shapiro, G. I.; Baum, A.; Himmelsbach, F.; Rettig, W. J.; Meyerson, M.; Solca, F.; Greulich, H.; Wong, K. K. *Oncogene.* **2008**, 27, 4702–4711.

27. Engelman, J. A.; Zejnullahu, F.; Gale, C. M.; Lifshits, E.; Gonzales, A. J.; Shimamura, T.; Zhao, F.; Vincent, P. W.; Naumov, G. N.; Bradner, J. E.; Althaus, I. W.; Gandhi, L.; Shapiro, G. I.; Nelson, J. M.; Heymach, J. V.; Meyerson, M.; Wong, K. K.; Jänne, P. A. *Cancer Res.* **2007**, 67, 11924–11932.

28. Zhou, W. J.; Ercan, D.; Chen, L.; Yun, C. H.; Li, D.; Capelletti, M.; Cortot, A. B.; Chirieac, L.; Iacob, R. E.; Padera, R.; Engen, J. R.; Wong, K. K.; Eck, M. J.; Gray, N. S.; Jä nne, P. A. *Nature*. **2009**, 462, 1070–1074.

29. Sos, M. L.; Rode, H. B.; Heynck, S.; Peifer, M.; Fischer, F.; Klüter, S.; Pawar,V. G.; Reuter, C.; Heuckmann, J. M.; Weiss, J.; Ruddigkeit, L.; Rabiller, M.; Koker, M.; Simard, J. R.; Getlik, M.; Yuza, Y.; Chen, T. H.; Greulich, H.; Thomas, R. K.; Rauh, D. *Cancer Res.* **2010**, 70, 868–874.

30.Kim, Y.; Ko, J.; Cui, Z.; Abolhoda, A.; Ahn, J. S.; Ou, S. H.; Ahn, M. J.; Park, K. *Mol. Cancer Ther.* **2012**, 11, 784–791.

31.Ercan, D.; Zejnullahu, K.; Yonesaka, K.; Xiao, Y.; Capelletti, M.; Rogers, A.; Lifshits, E.; Brown, A.; Lee, C.; Christensen, J. G.; Kwiatkowski, D. J.; Engelman, J. A.; Jä nne, P. A. *Oncogene.* **2010**, 29, 2346–2356.

32. Wang, S.; Cang, S.; Liu, D. *J. Hematol Oncol.* **2016**, 9, 34.

33.Yu, H. A.; Tian, S. K.; Drilon, A. E.; Borsu, L.; Riely, G. J.; Arcila, M. E.; Ladanyi, M. *JAMA Oncology.* **2015**, 1, 982-984.

34.Niederst, M. J.; Hu, H.; Mulvey, H. E.; Lockerman, E. L.; Garcia, A. R.; Piotrowska, Z.; Sequist, L. V.; Engelman, J. A. *Clinical Cancer Research* **2015**, 21, 3924-3933

35.Patel, H. M.; Rane, R.; Thapliyal, N.; Palkar, M.; Shaikh, M.; Karpoormath, R. *Anticancer Agents Med. Chem.* **2015**,15, 988-1011.

36.Patel, H. M.; Bari, P.; Karpoormath, R.; Noolvi, M.; Thapliyal, N.; Surana, S.; Jain, P. *RSC Adv.* **2015**, 5, 56724-56771.

37.Thakor, V.; Poddar, M.; Patel, H. M.; Dey, S.; Manjula, S. N.; Subbarao, M.; Pawara, R. *RSC Adv.* **2016**, 6, 79166-79179.

38.Noolvi, M. N.; Patel, H. M. *Arab. J. Chem.* **2013**, 6, 35-48.

39.Patel, H. M.; Surana, S.; Shirkhedkar, A.; Kulkarni, A.; Pardeshi, C. V. *RSC Adv.* **2016**, 6, 44435-44455.

40.Alley, M. C.; Scudiero, D. A.; Monks, P. A.; Hursey, M. L.; Czerwinski, M. J.; Fine, D. L.; Abbott, B. J.; Mayo, J. G.; Shoemaker, R. H.; Boyd, M. R. *Cancer Res.* **1988**, 48,589-601.

41. Grever, M. R.; Schepartz, S. A.; Chabner, B. A. *Semin. Oncol.* **1992**,19,622-638.

42.Boyd, M. R.; Paull, K. D. *Drug Develop. Res.* **1995**, 19, 91-109.

43.Rostom, S. A. F. *Bioorg. Med. Chem.* **2006**, 14, 6475–6485.

44. Shao, J.; Chen, E.; Shu,K.; Chen, W.; Zhang, G.; Yu, Y. *Bioorg. Med. Chem.* **2016**, *24*, 3359-3370

45.Halgren, T.A.; Murphy, R.B.; Friesner, R.A.; Beard, H.S.; Frye, L.L.; Pollard, W.T.; Banks, J.L. *J. Med. Chem.* **2004**, 47,1750–1759.

46. Friesner, R.A.; Banks, J.L.; Murphy. R. B.; Halgren, T.A.; Klicic, J.J.; Mainz, D.T.; Repasky, M.P.; Knoll, E.H.; Shelley, M.; Perry, J.K.; Shaw, D.E.; Francis, P.; Shenkin, P.S. *J. Med. Chem.* 2004, 47, 1739–1749.

47.Sherman, W.; Day, T.; Jacobson, M. P.; Friesner, R.A. *J. Med. Chem.* **2006**, 49, 534–553.

48. http://www.rcsb.org/pdb/explore/explore.3B8Q.

49.QikProp, version 9.0, Schrodinger, LLC, New York, NY, **2010**.

50.Ligprep, version 9.0, Schrodinger, LLC, New York, NY, **2010**.

Supplementary Information

Design and Synthesis of Quinazolinones as EGFR inhibitors to Overcome EGFR Resistance Obstacle

Harun M. Patel [a] *, Rahul Pawara [a], Azim Ansari [a], Malleshappa Noolvi [b], Sanjay Surana [a]

[a] Department of Pharmaceutical Chemistry, R. C. Patel Institute of Pharmaceutical Education and Research, Shirpur, District Dhule-425 405, Maharashtra, India

[b] Department of Pharmaceutical Chemistry, Shree Dhanvantary Pharmacy College, Kim (Surat)-3941110, Gujrat, India

Corresponding Author*

Tel: +91-8806621544; Email:hpatel_38@yahoo.com

Figure 1S. IR Spectra of Compound **17**

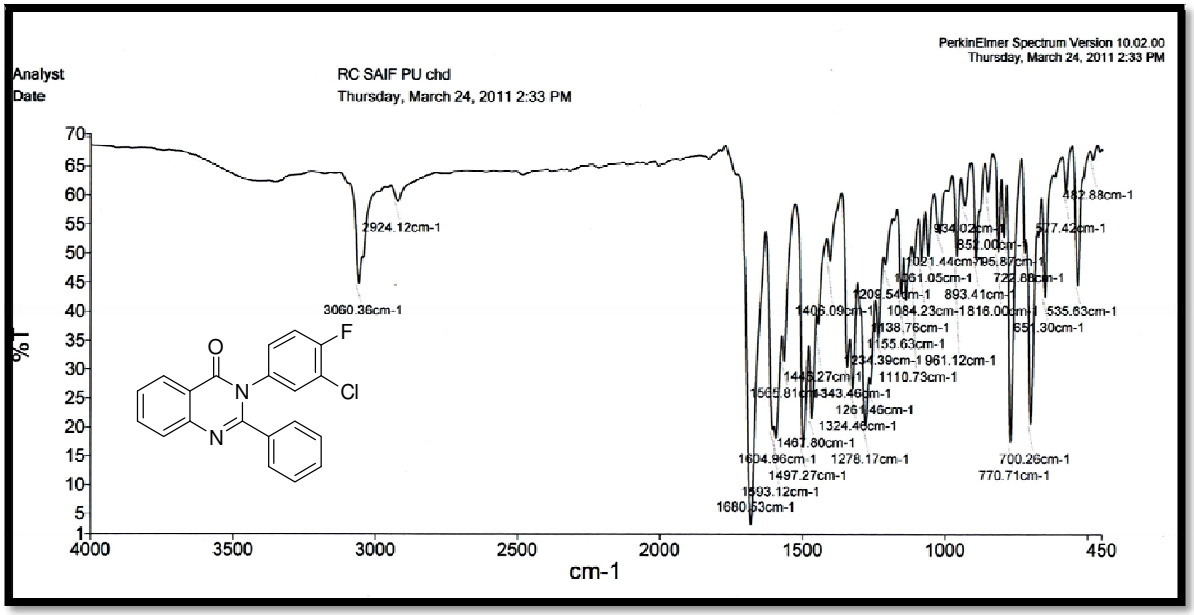

Figure 2S. [1]HNMR Spectrum of Compound **17**

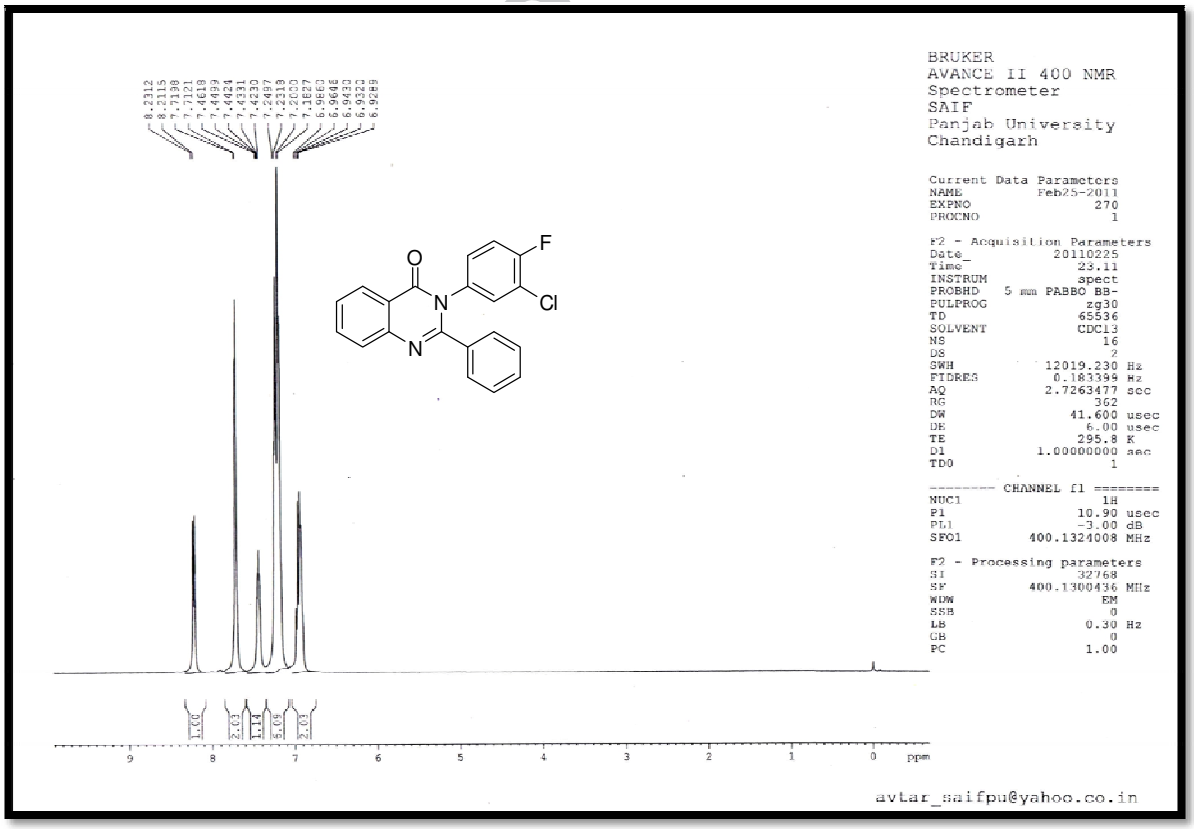

Figure 3S. ^{13}C NMR Spectrum of Compound **17**

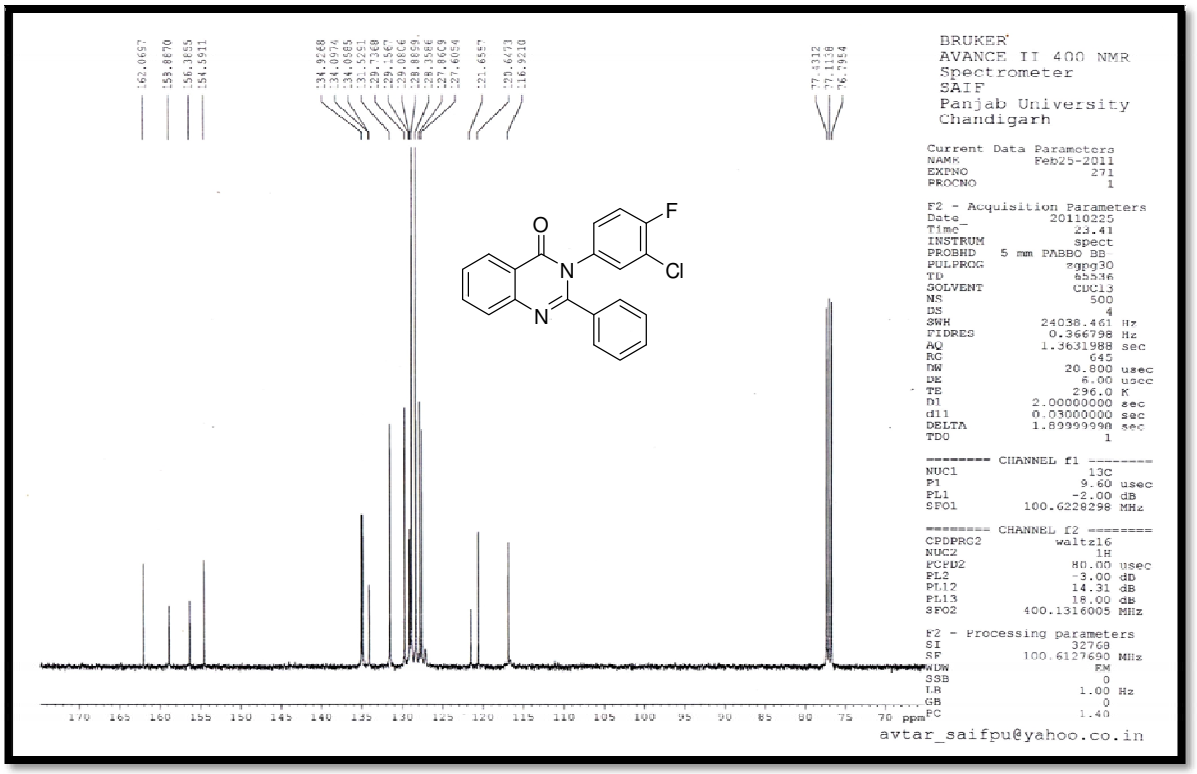

Figure 4S. Mass spectrum of Compound **17**

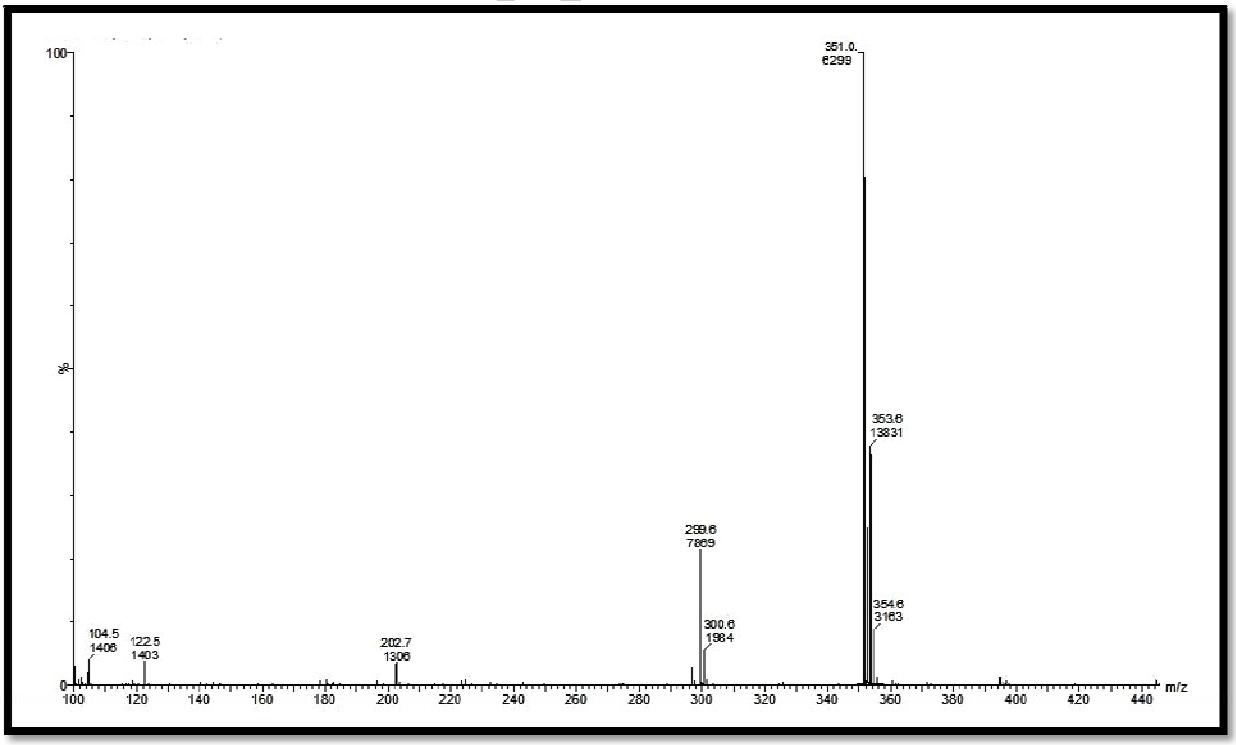

Figure 5S. IR Spectra of Compound **31**

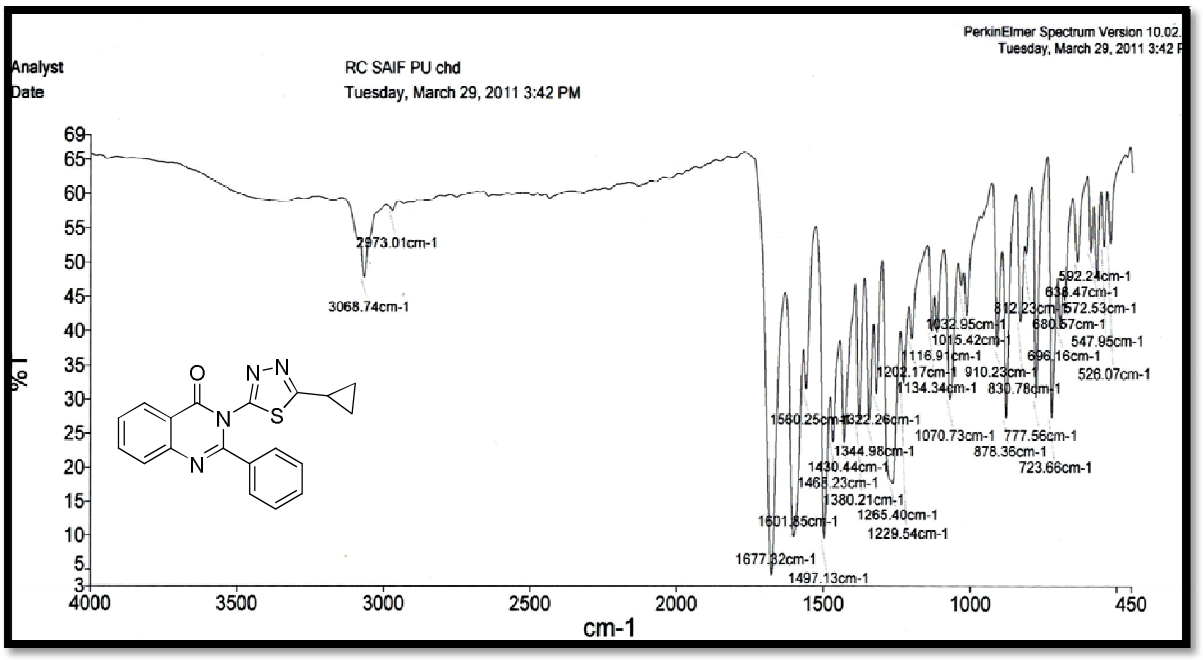

Figure 6S. [1]HNMR Spectrum of Compound **31**

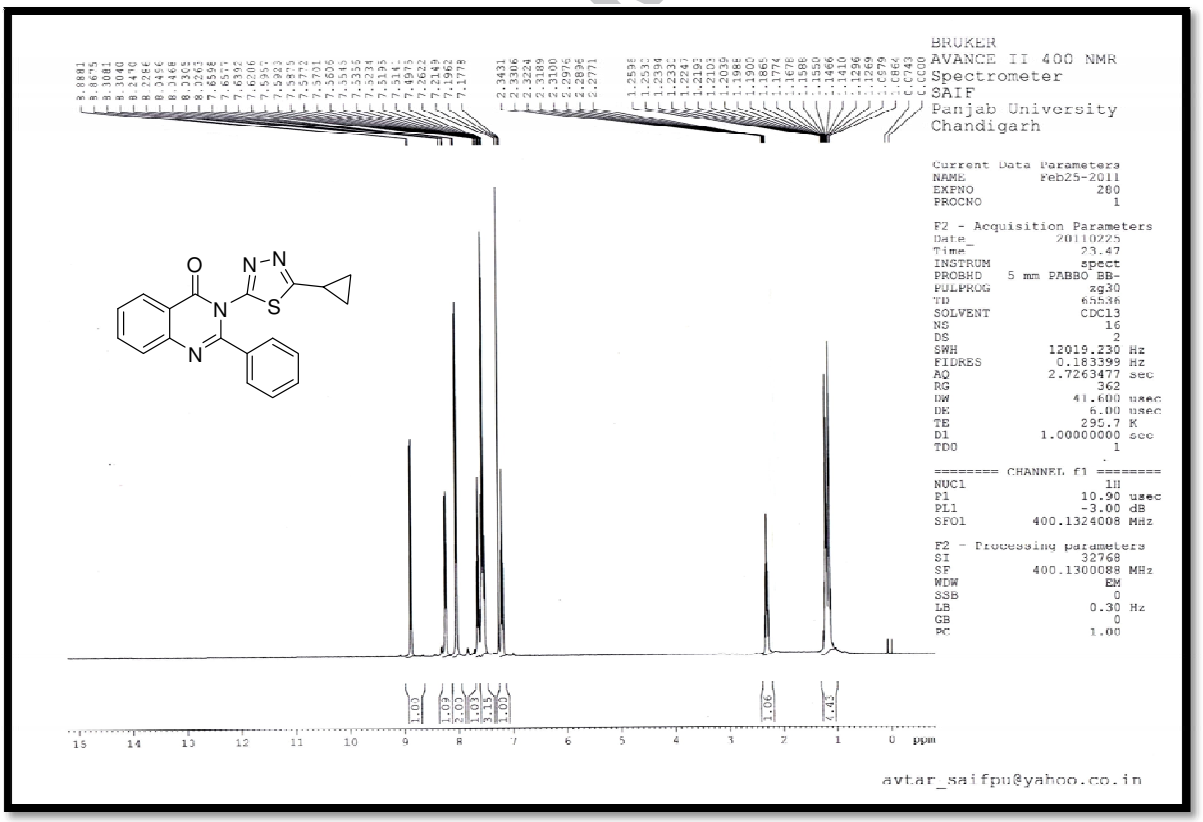

Figure 7S. ^{13}C NMR Spectrum of Compound **31**

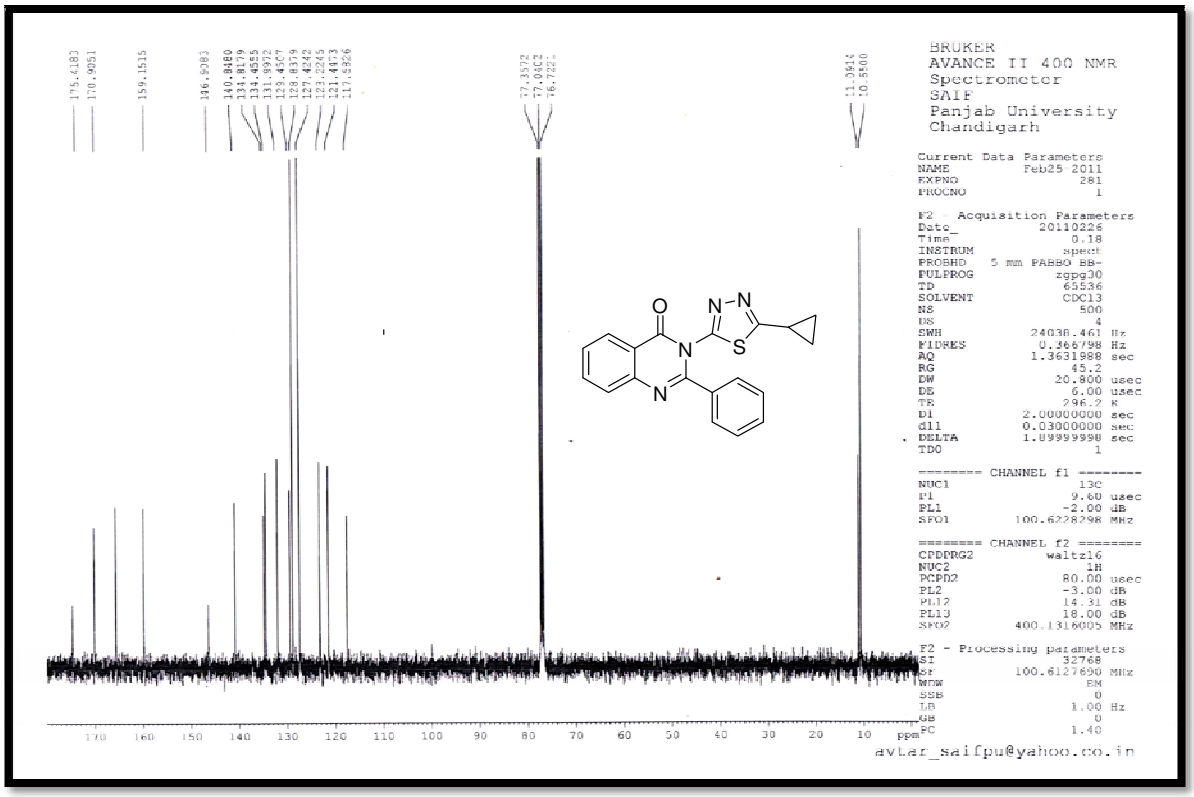

Figure 8S. Mass spectrum of Compound **31**

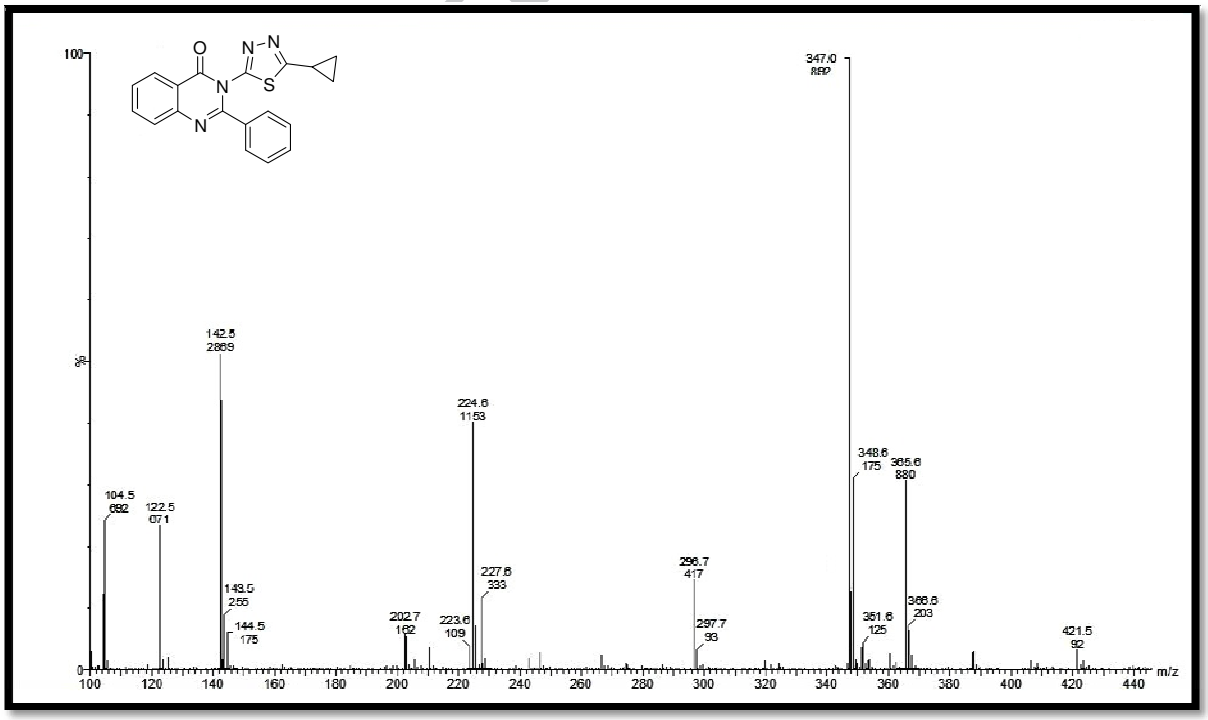

Figure 9S. IR Spectra of Compound **48**

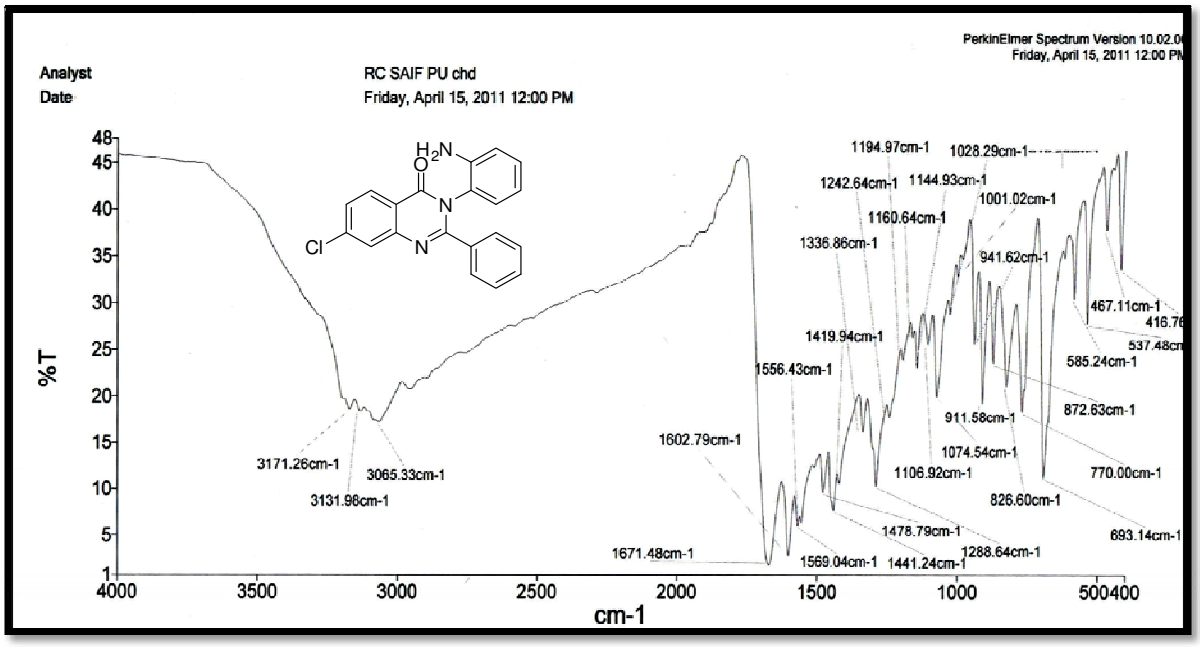

Figure 10S. [1]HNMR Spectrum of Compound **48**

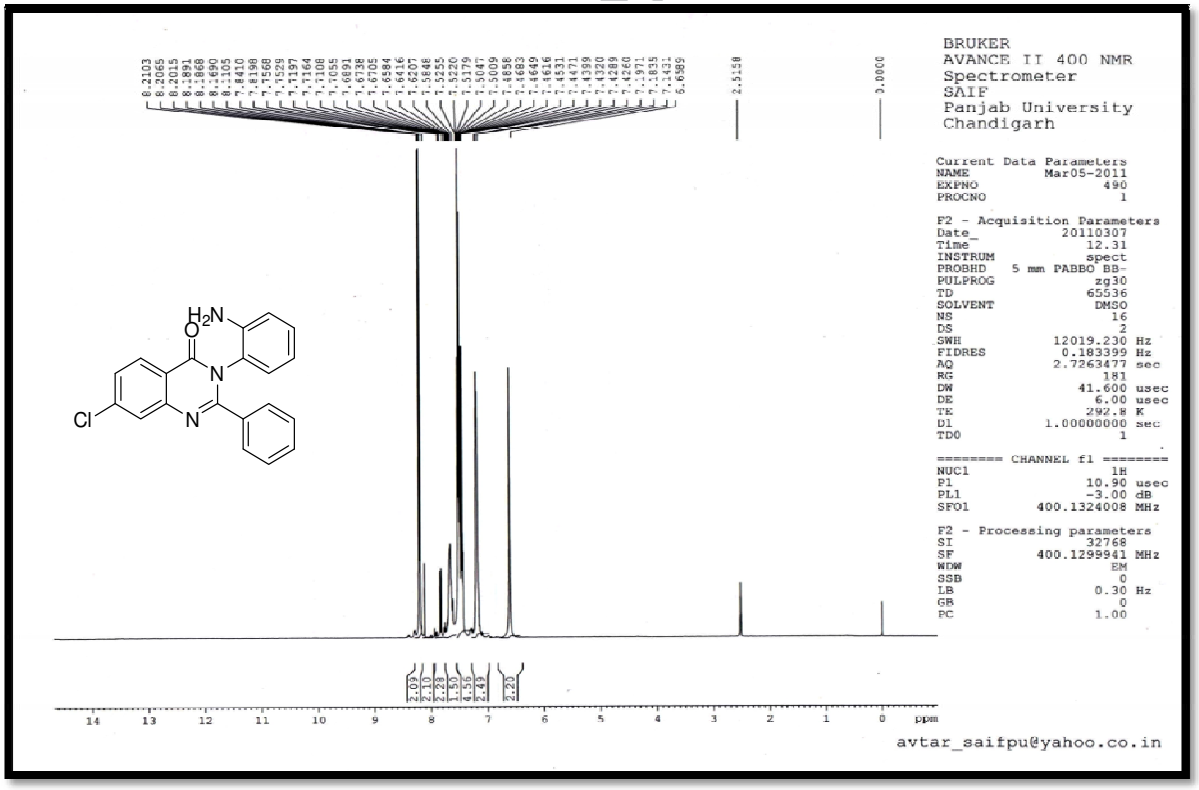

Figure 11S. ^{13}C NMR Spectrum of Compound **48**

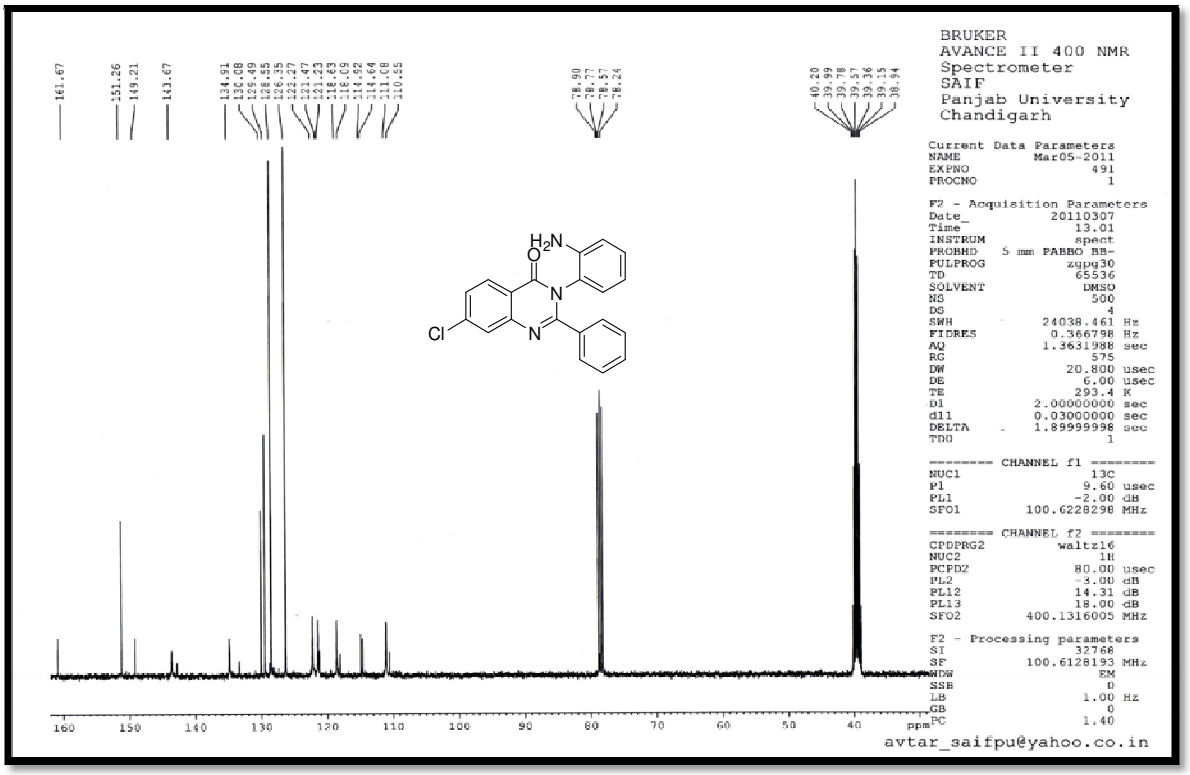

Figure 12S. Mass spectrum of Compound **48**

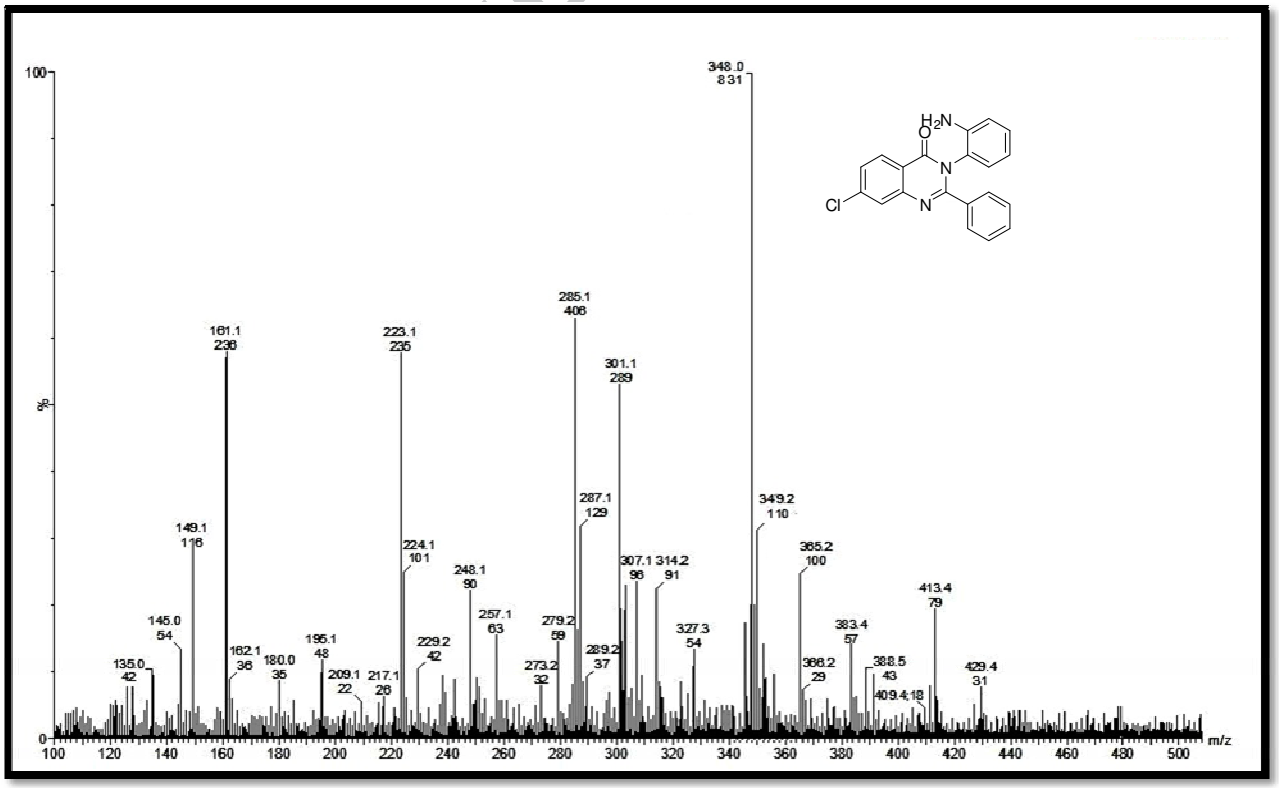

Figure 13S. IR Spectra of Compound **51**

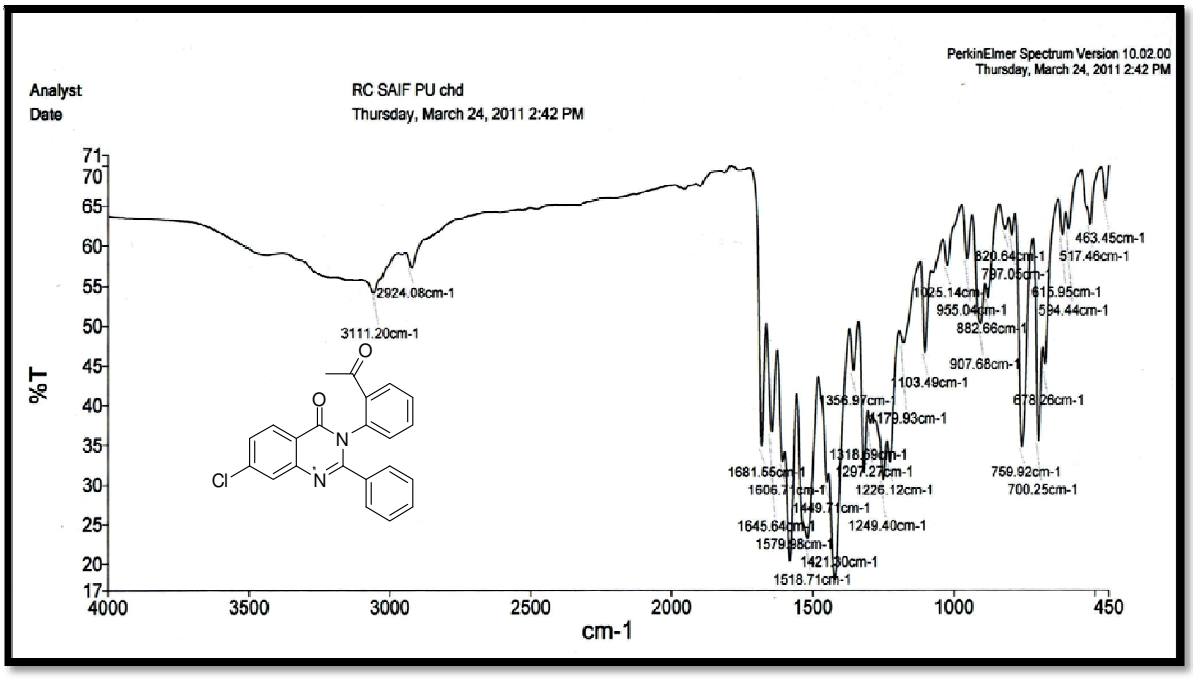

Figure 14S. [1]HNMR Spectrum of Compound **51**

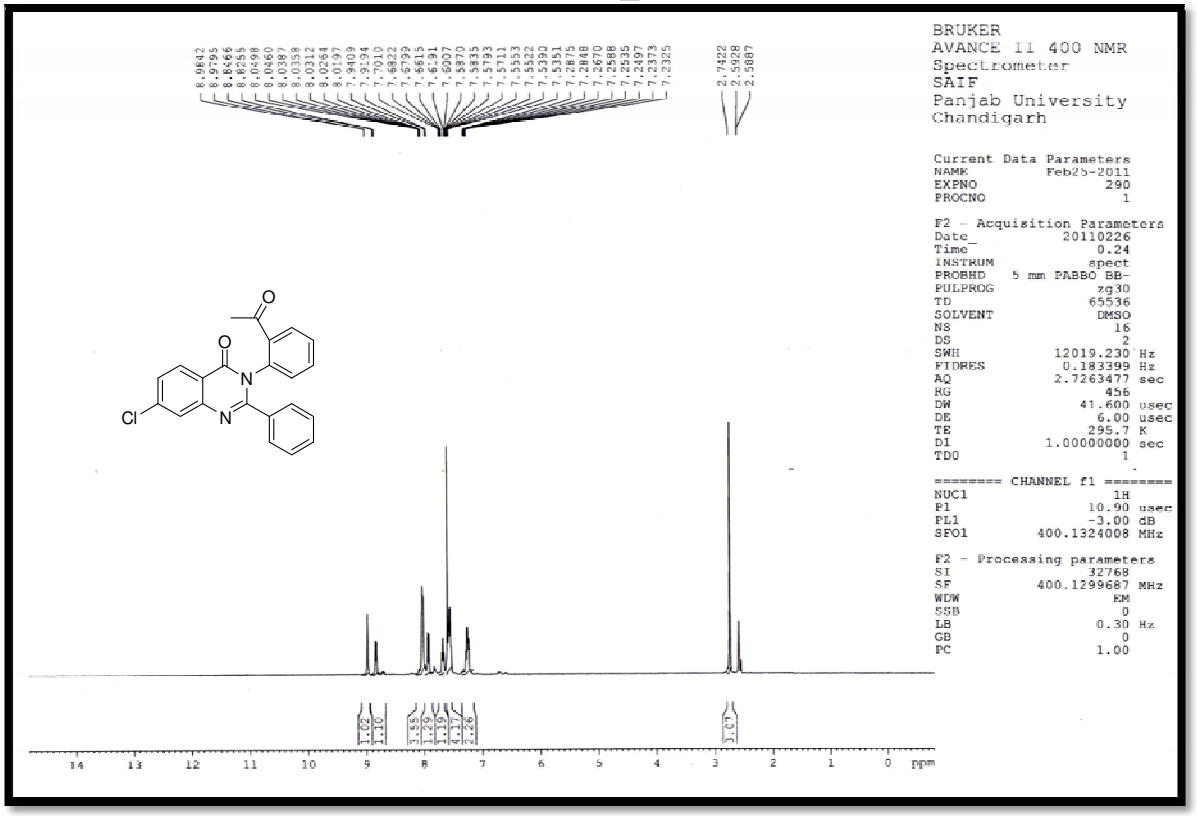

Figure 15S. ^{13}C NMR Spectrum of Compound **51**

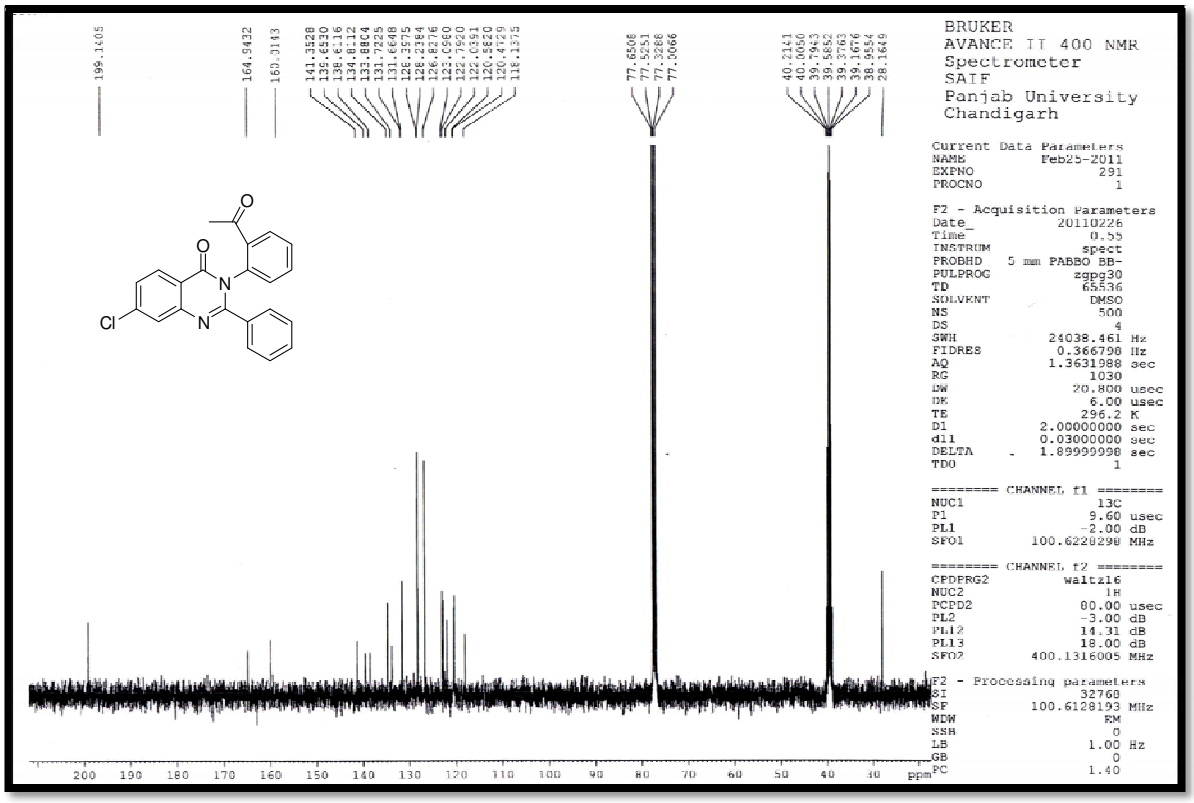

Figure 16S. Mass spectrum of Compound **51**

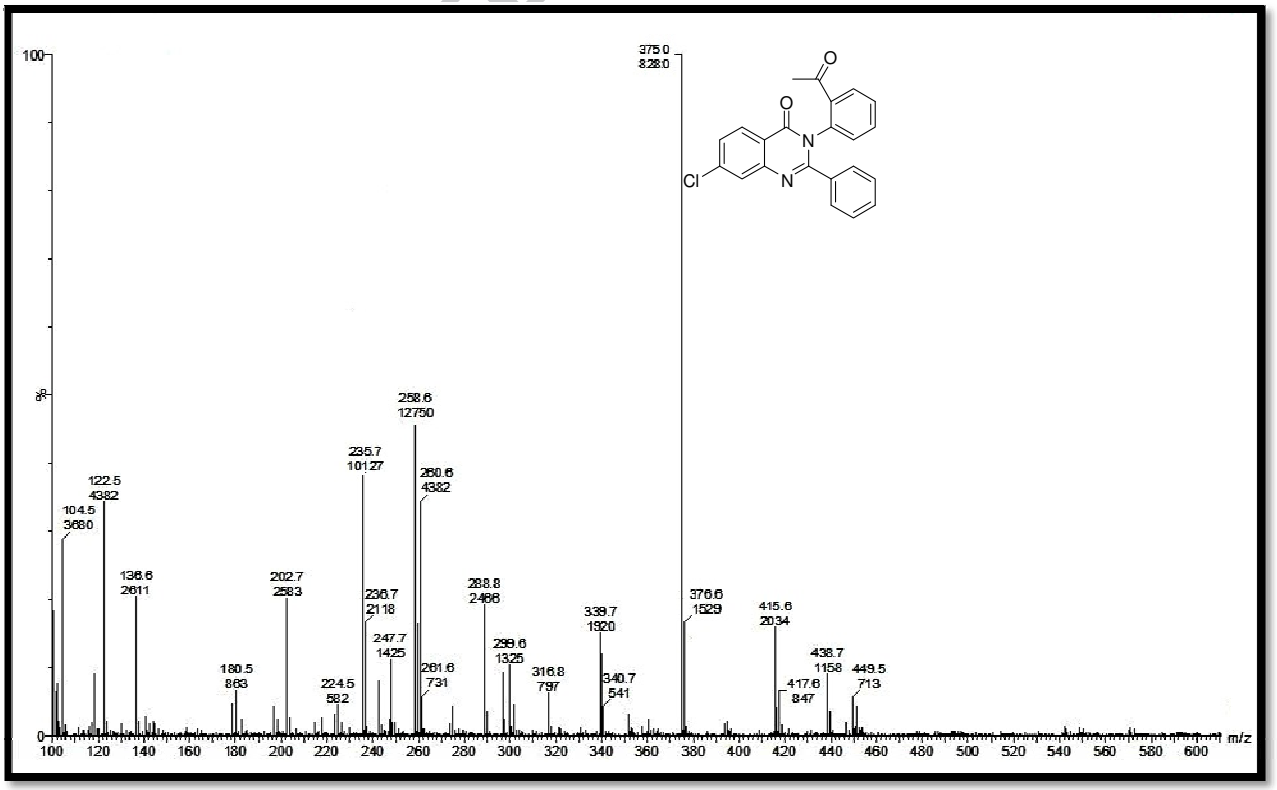

Figure 17S. IR Spectra of Compound **55**

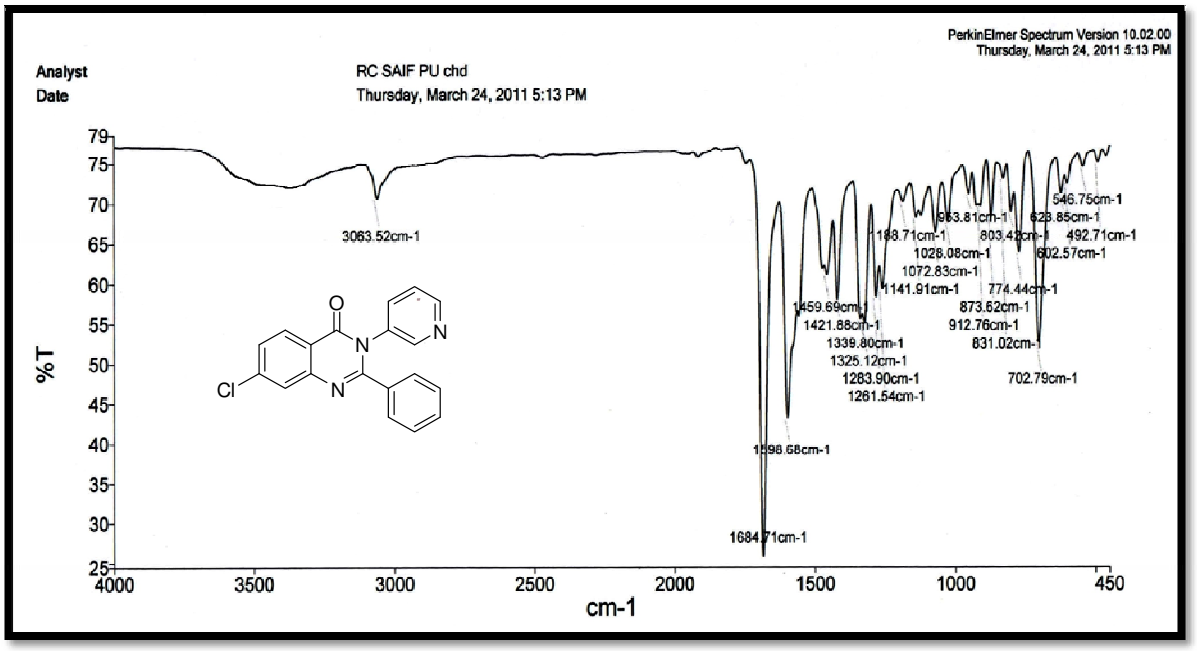

Figure 18S. [1]HNMR Spectrum of Compound **55**

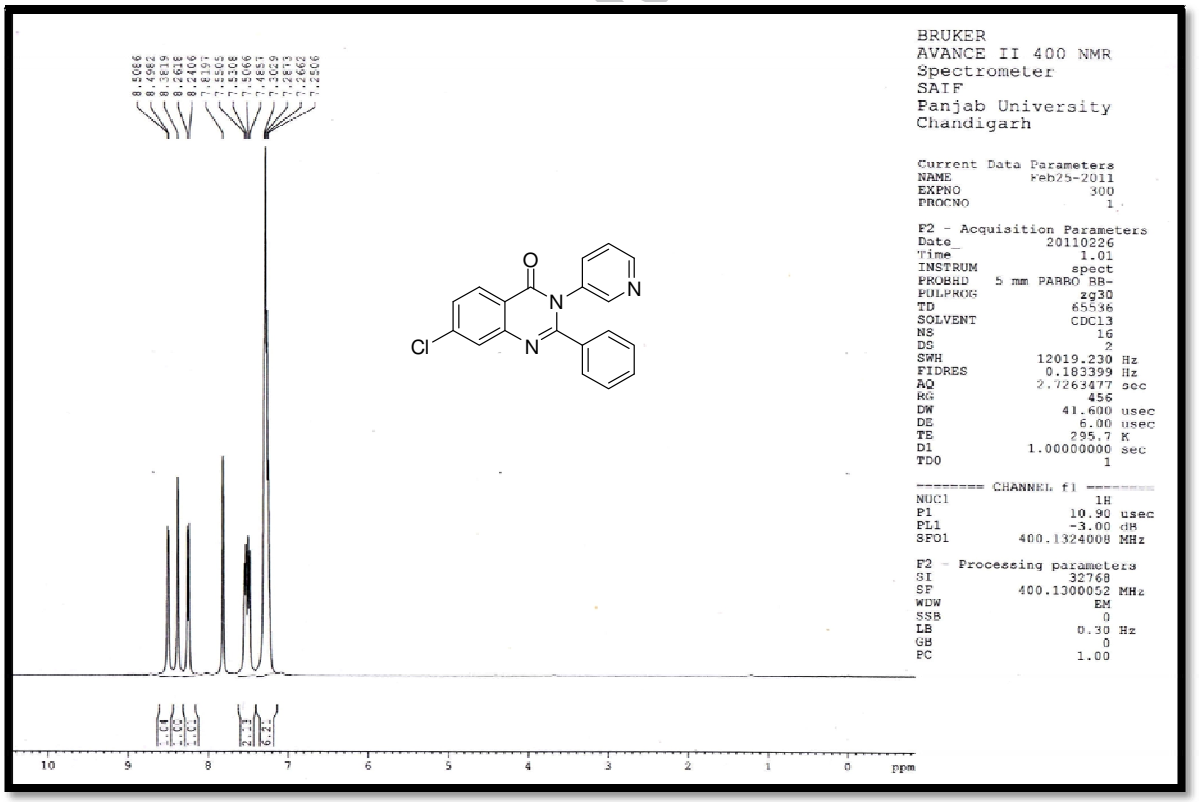

Figure 19S. ^{13}C NMR Spectrum of Compound **55**

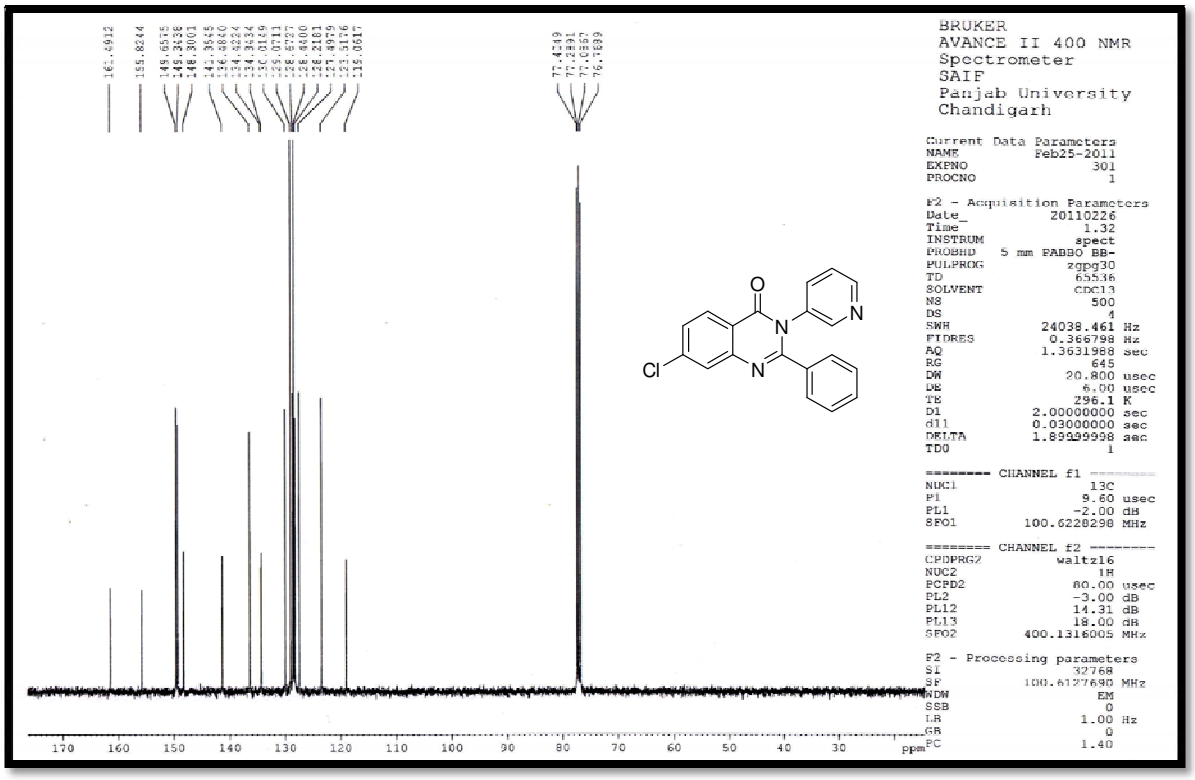

Figure 20S. Mass spectrum of Compound **55**

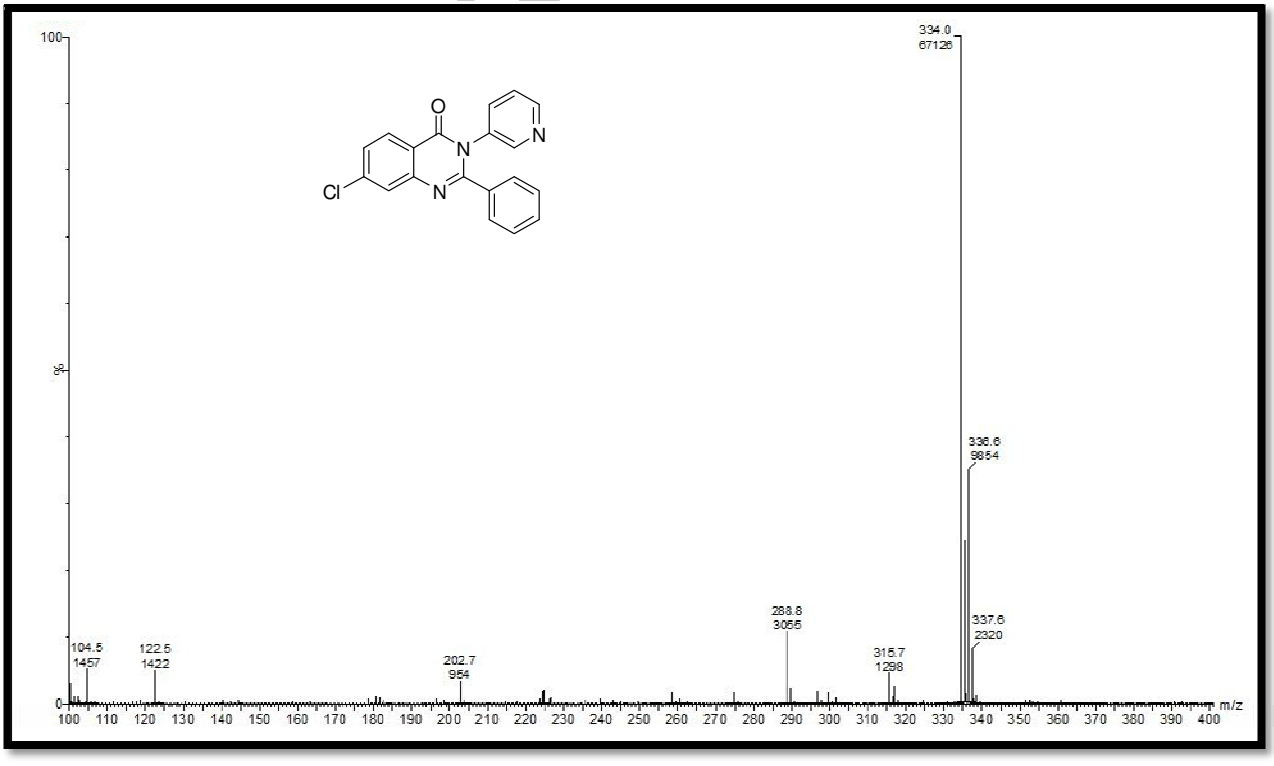

Figure 21S. IR Spectra of Compound **60**

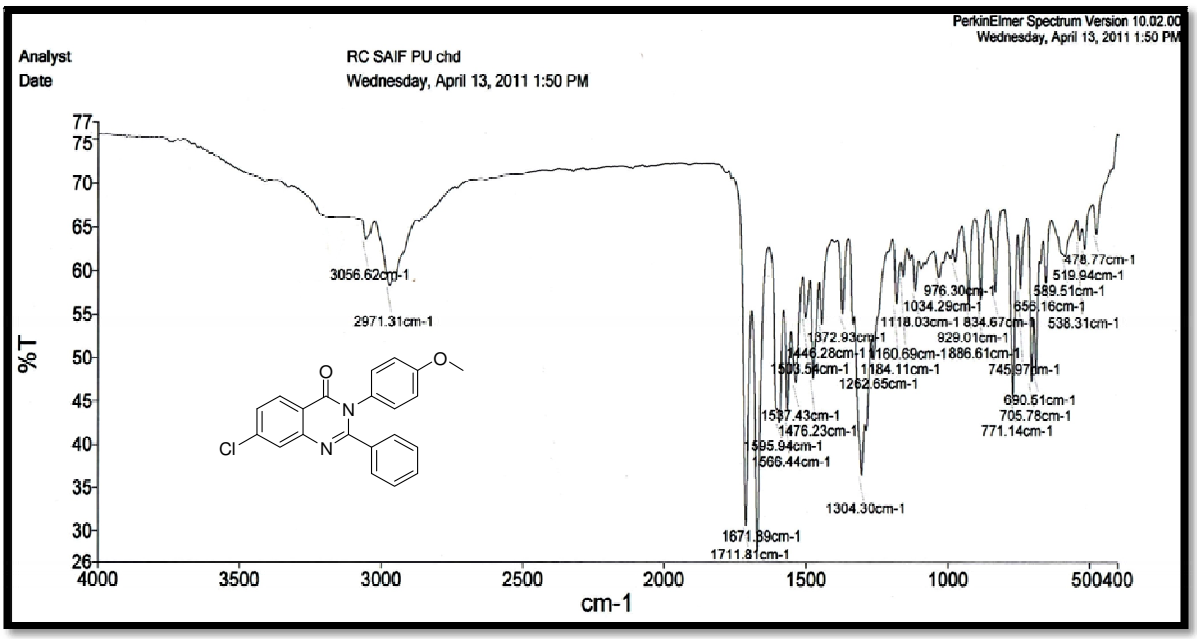

Figure 22S. [1]HNMR Spectrum of Compound **60**

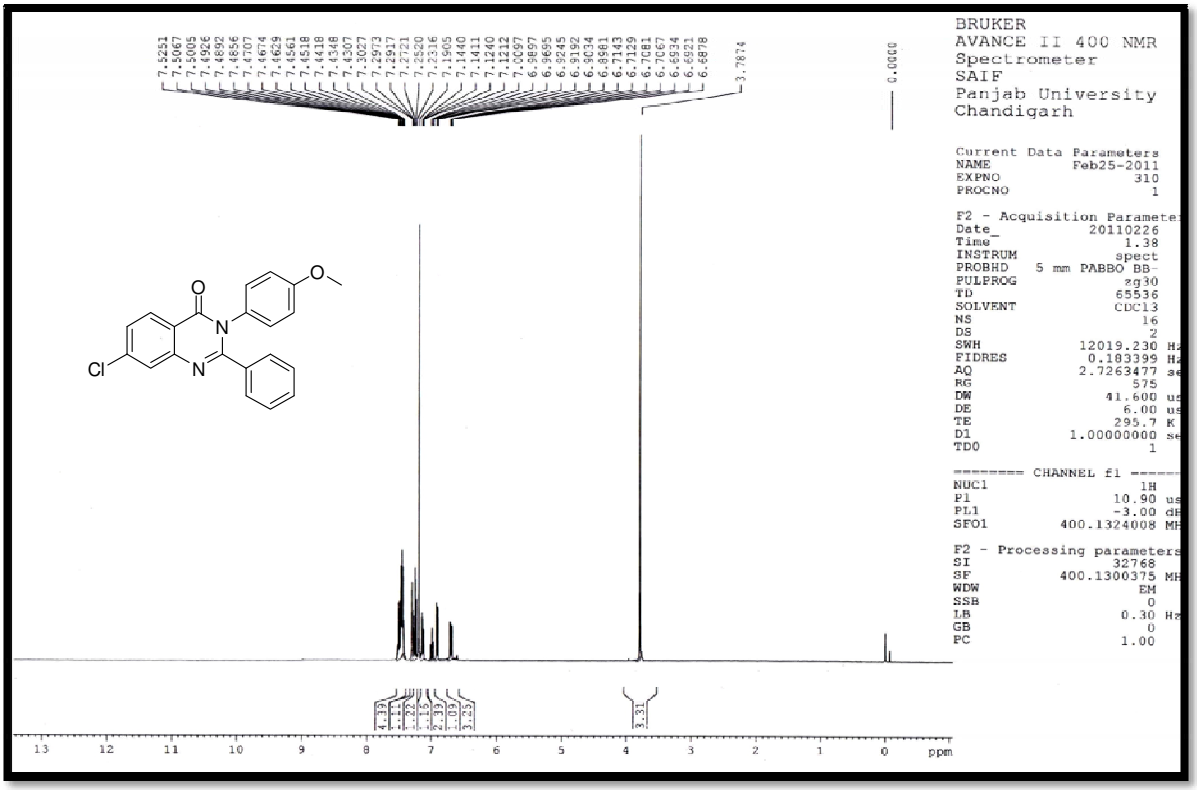

Figure 23S. ^{13}C NMR Spectrum of Compound **60**

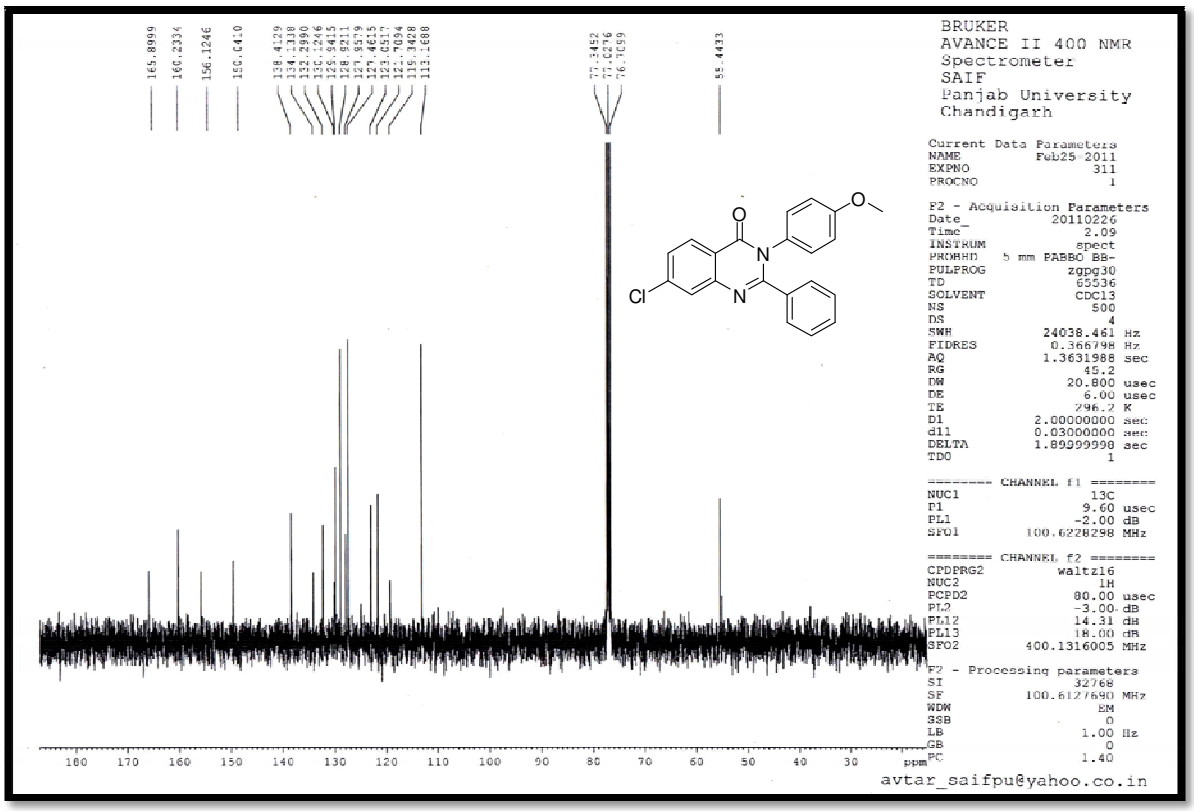

Figure 24S. Mass spectrum of Compound **60**

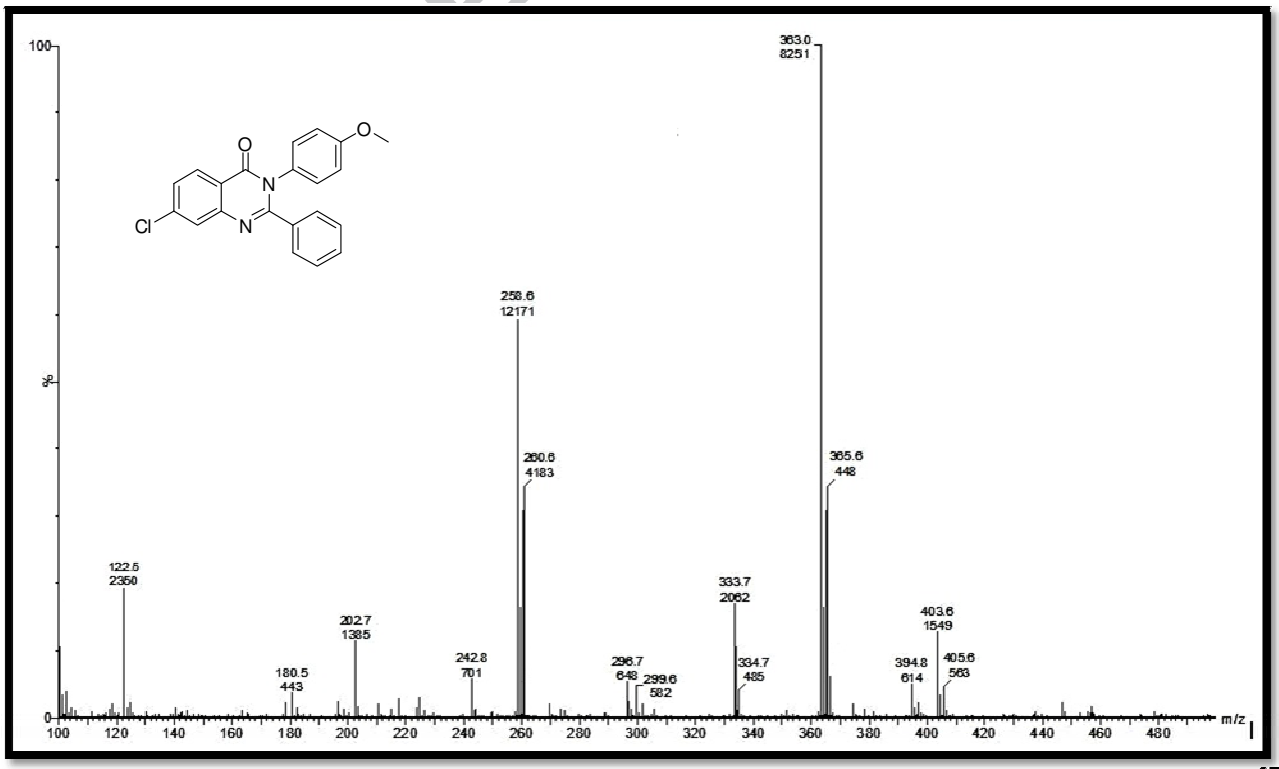

Figure 25S. IR Spectra of Compound **86**

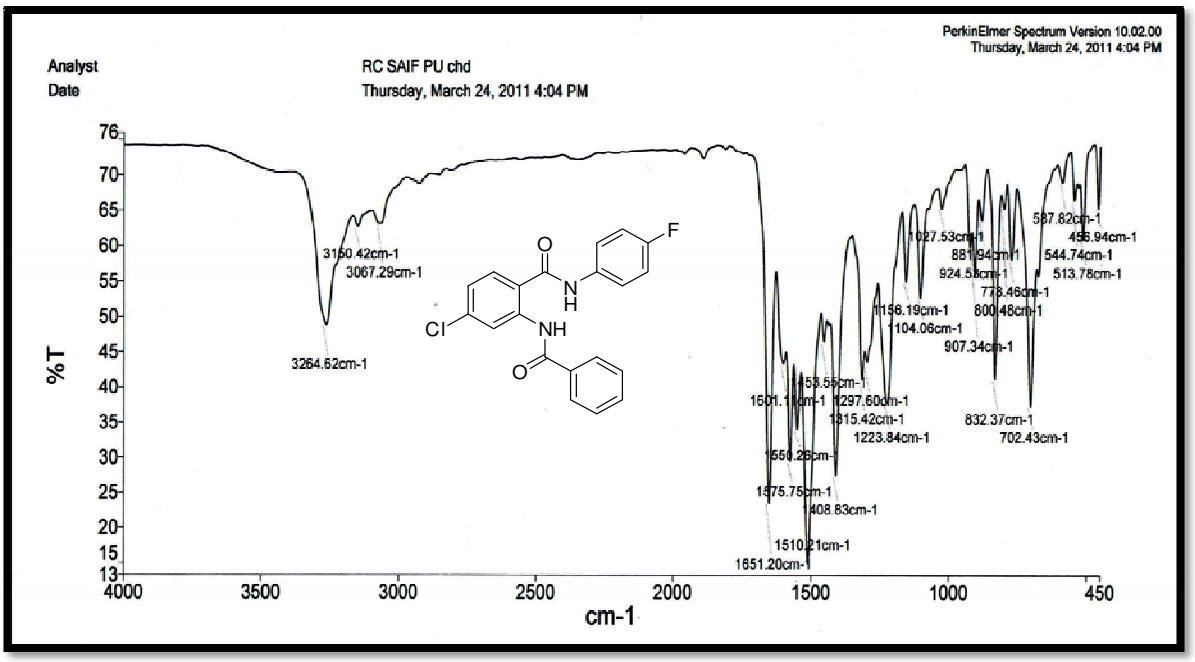

Figure 26S. [1]HNMR Spectrum of Compound **86**

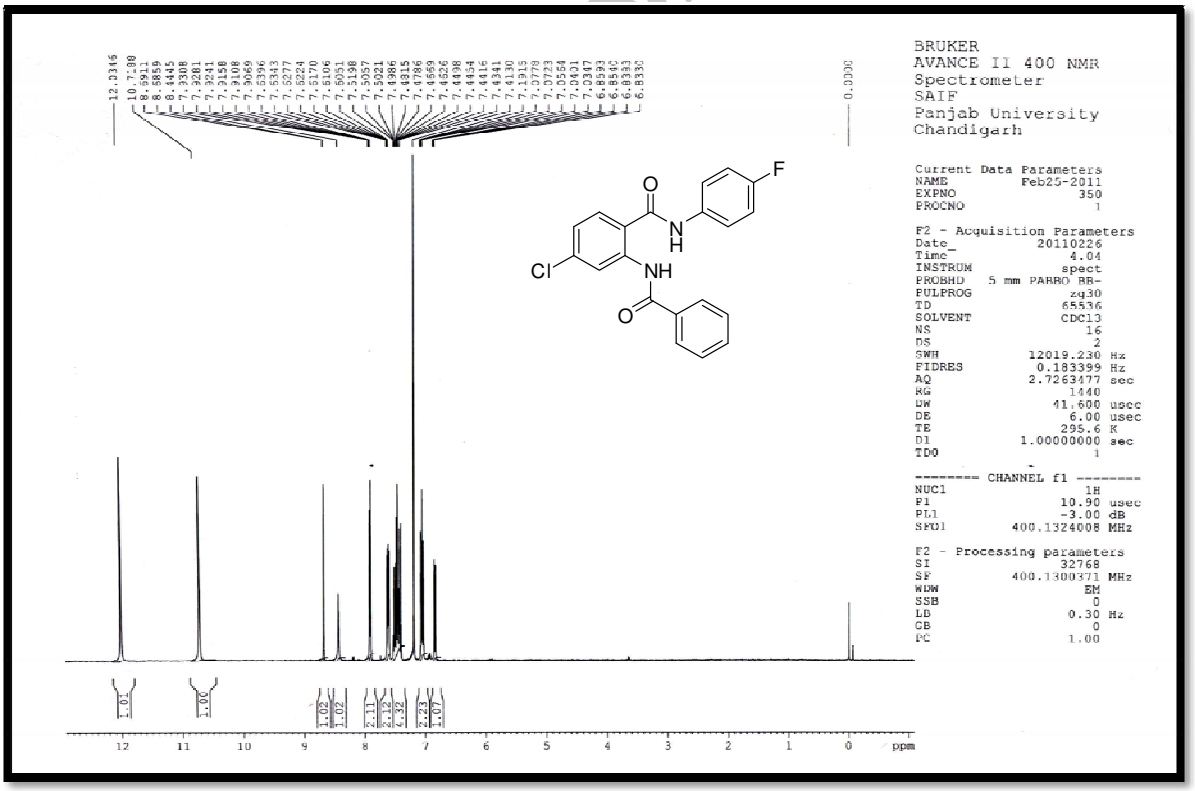

Figure 27S. ^{13}C NMR Spectrum of Compound **86**

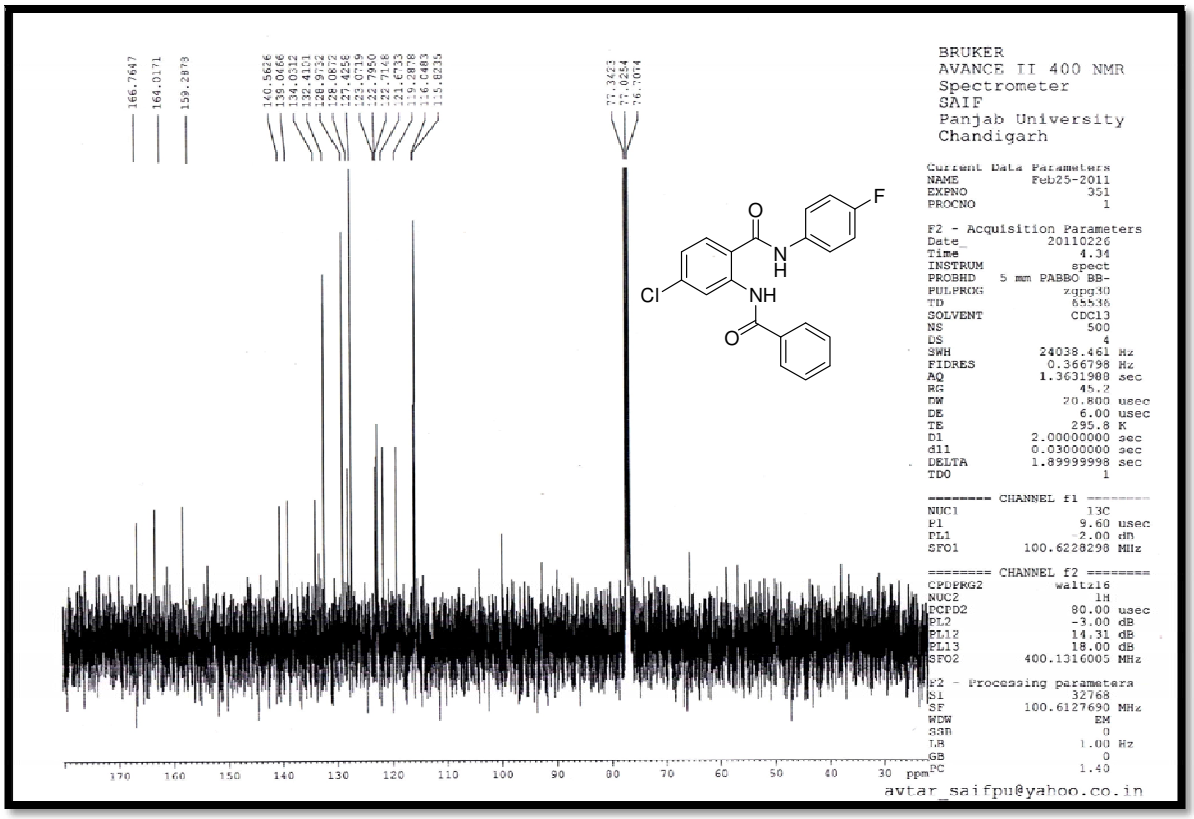

Figure 28S. Mass spectrum of Compound **86**

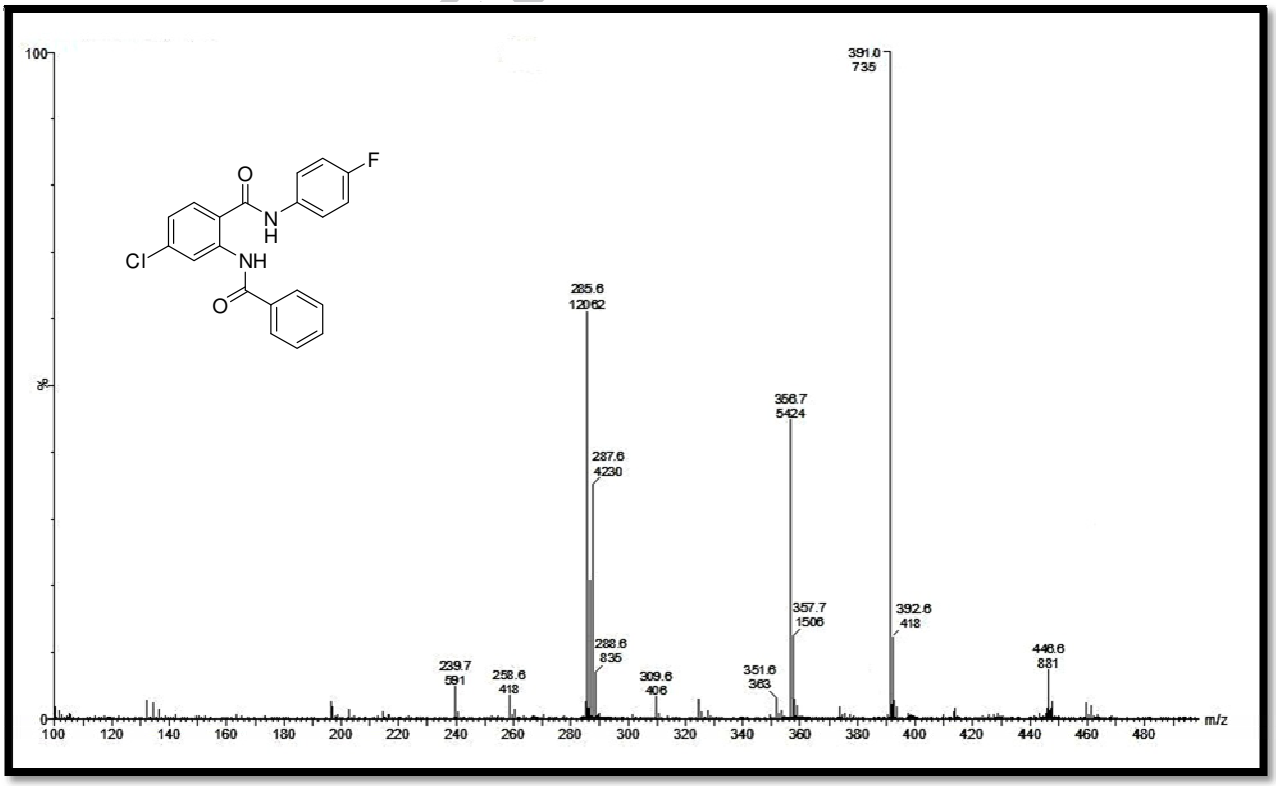

Figure 29S. IR Spectra of Compound **94**

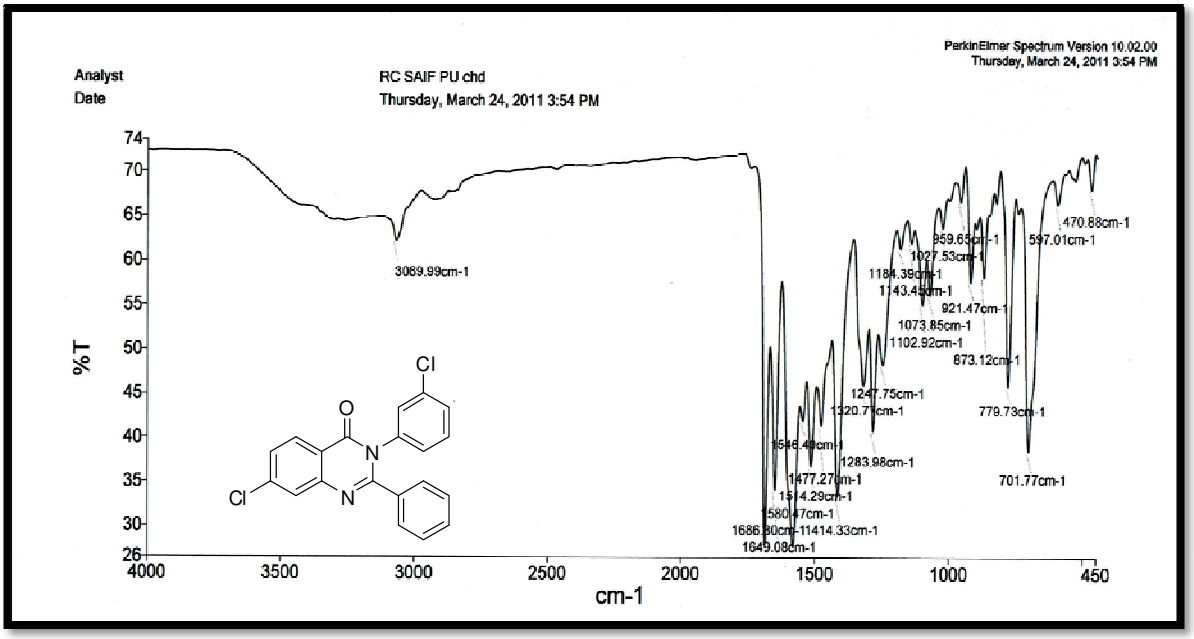

Figure 30S. [1]HNMR Spectrum of Compound **94**

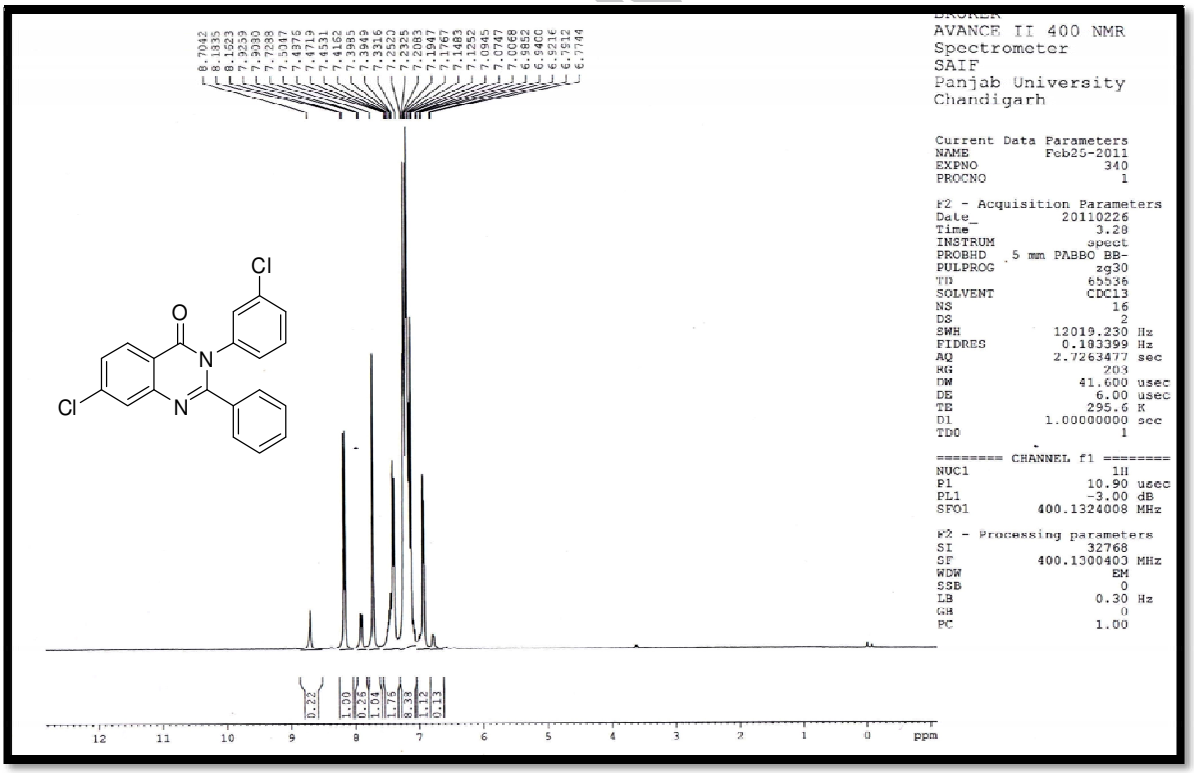

Figure 31S. ^{13}C NMR Spectrum of Compound **94**

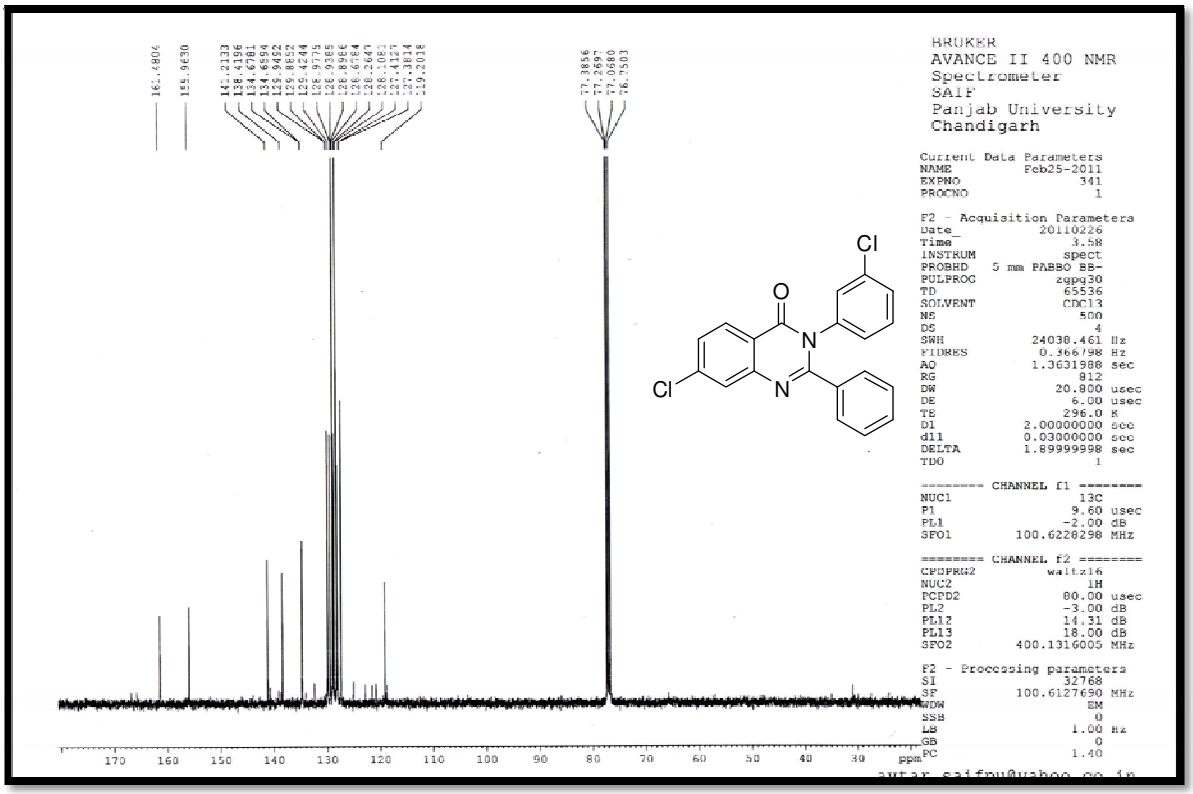

Figure 32S. Mass spectrum of Compound **94**

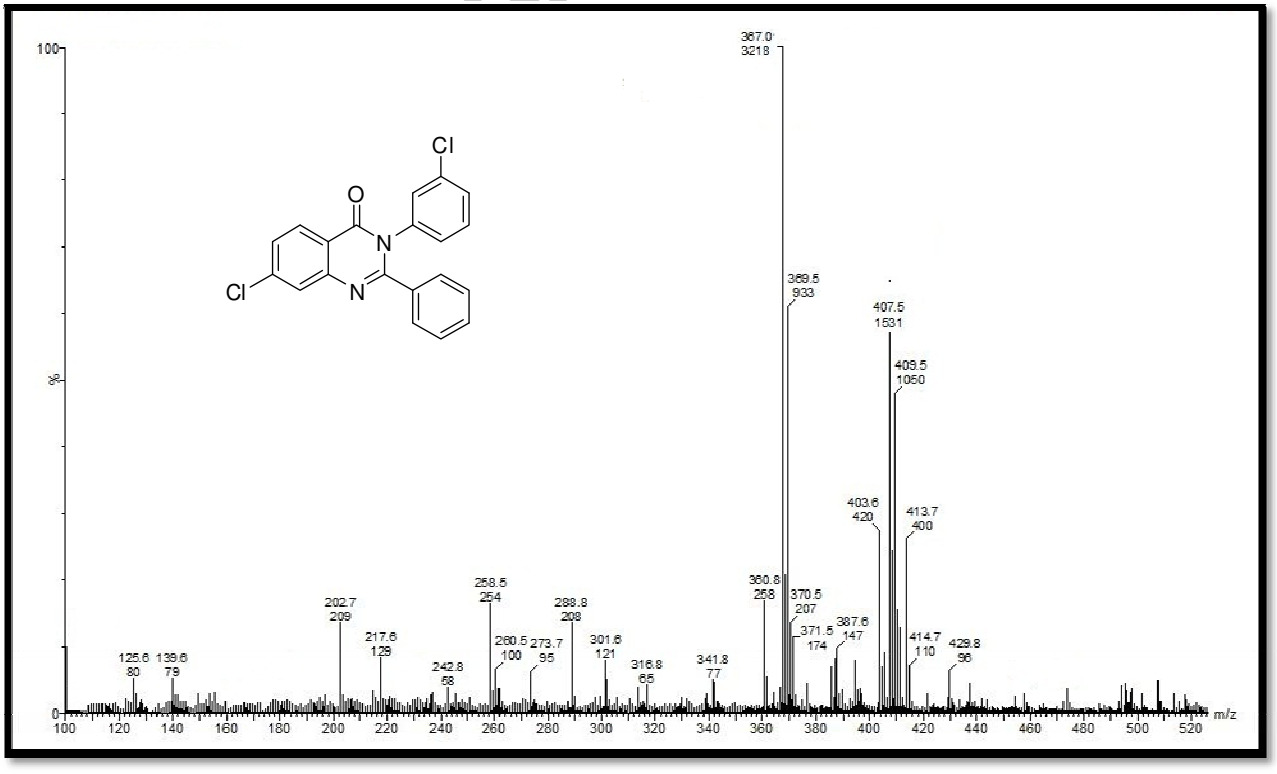

Graphical Abstract

Design and Synthesis of Quinazolinones as EGFR inhibitors to Overcome EGFR Resistance Obstacle

Harun M. Patel, Rahul Pawara, Azim Ansari, Malleshappa Noolvi , Sanjay Surana